Summer 2011

Influence of rear wheel tire type on wheelchair propulsion biomechanics

Mathew Yarossi
New Jersey Institute of Technology

Copyright Warning & Restrictions

The copyright law of the United States (Title 17, United States Code) governs the making of photocopies or other reproductions of copyrighted material.

Under certain conditions specified in the law, libraries and archives are authorized to furnish a photocopy or other reproduction. One of these specified conditions is that the photocopy or reproduction is not to be "used for any purpose other than private study, scholarship, or research." If a, user makes a request for, or later uses, a photocopy or reproduction for purposes in excess of "fair use" that user may be liable for copyright infringement,

This institution reserves the right to refuse to accept a copying order if, in its judgment, fulfillment of the order would involve violation of copyright law.

Please Note: The author retains the copyright while the New Jersey Institute of Technology reserves the right to distribute this thesis or dissertation

Printing note: If you do not wish to print this page, then select "Pages from: first page # to: last page #" on the print dialog screen

ABSTRACT

INFLUENCE OF REAR WHEEL TIRE TYPE ON WHEELCHAIR PROPULSION BIOMECHANICS

by
Mathew Yarossi

The objective of this study was to determine how rear wheel tire type affects wheelchair propulsion mechanics. Four persons with paraplegia and four persons with tetraplegia propelled their own wheelchairs on a roller system at self-selected speed using five different pairs of tires. Upper limb and trunk kinematics, perceived exertion, stroke pattern and the temporal characteristics of propulsion were measured. When using pneumatic (air filled) tires, with lower rolling resistance, participants had lower push frequency ($p < .05$), higher self selected speed ($p < .05$), less perceived exertion, less shoulder internal rotation, and a longer push stroke than when using solid, high rolling resistance tires. As rolling resistance increased, participants experienced negative changes in propulsion characteristic that contradicted current clinical practice guidelines for upper limb preservation following spinal cord injury. In addition, kinematics with solid, high rolling resistance tires were similar to those described during uphill or over carpet propulsion. In order to avoid unnecessary strain on the upper limbs and unwanted changes in propulsion biomechanics, wheelchair users, clinicians, and researchers should consider the use of lower rolling resistance, pneumatic rear tires.

INFLUENCE OF REAR WHEEL TIRE TYPE ON WHEELCHAIR PROPULSION BIOMECHANICS

by
Mathew Yarossi

A Thesis
Submitted to the Faculty of
New Jersey Institute of Technology
in Partial Fulfillment of the Requirements for the Degree of
Master of Science in Biomedical Engineering

Department of Biomedical Engineering

August 2011

APPROVAL PAGE

INFLUENCE OF REAR WHEEL TIRE TYPE ON WHEELCHAIR PROPULSION BIOMECHANICS

Mathew Yarossi

Dr. Trevor Dyson-Hudson, Thesis Co-Advisor Director of Spinal Cord Injury Outcomes, Kessler Foundation Research Center	Date
Dr. Richard Foulds, Thesis Co-Advisor Associate Professor of Biomedical Engineering, NJIT	Date
Dr. Gail Forrest, Thesis Committee Member Director of Human Performance and Movement Analysis Laboratory, Kessler Foundation Research Center	Date
Dr. Sergei Adamovich, Thesis Committee Member Associate Professor of Biomedical Engineering, NJIT	Date

BIOGRAPHICAL SKETCH

Author: Mathew Yarossi

Degree: Master of Science

Date: May 2011

Undergraduate and Graduate Education:

- Master of Science in Biomedical Engineering,
  New Jersey Institute of Technology, Newark, NJ, 2011

- Bachelor of Science in Biomedical Engineering,
  Northwestern University, Evanston, IL, 2004

Major: Biomedical Engineering

"Whatever you do, take care of your shoes."
- Trey Anastasio

I would like to dedicate this thesis to my family for always being supportive of my academic pursuits however foolish they may be.

ACKNOWLEDGEMENT

I would first like to thank Dr. Richard Foulds, Dr. Sergei Adamovish, Dr. Trevor Dyson-Hudson, and Dr. Gail Forrest, for actively participating in my committee and providing excellent mentorship and kind support throughout the process. A would like to also thank my colleagues at the Kessler Foundation including Arvind Ramanujam, Karen Nolan and Milda Woods for their support and sharing of scientific knowledge. Lastly, I would like to express my deepest appreciation to Dr. Sue Ann Sisto for giving me a chance to work at the Kessler Foundation, and for her assistance and guidance throughout the study.

A very special thank you goes to Andrew Kwarciak, without whom this research would have not been possible. The study presented in this thesis was the collaborative idea of Andrew and myself, developed while working as engineers at the Kessler Foundation Research Center on a project titled, "Predictors of Shoulder Pain and Pathology during Manual Wheelchair Propulsion in Individuals with Tetraplegia". The goal of this study, sponsored by the New Jersey Commission on Spinal Cord Injury Research, was to examine the biomechanics (kinematics, kinetics and electromyography) of wheelchair propulsion that show the greatest association to pain and pathology. In order to measure pushrim kinetics the SmartWHEEL instrumented wheelchair wheel was used, replacing the participants' wheel during testing. During the testing of the first four participants, Andrew and I observed that participants pushed very differently with the instrumented wheel than with their own wheel. Several participants commented the SmartWHEEL seemed more difficult to push. Though initially we dismissed these

differences as unavoidable due to the heavier weight of the instrumented wheel, we also observed the tires commonly used by our participants were very different than the one supplied with the SmartWHEEL. Most participants were using a pneumatic tire while the tire being used in the experiment was made from solid foam. A two-part study was devised to test the effect of tire type on the manual wheelchair user. Part one of the study involved studying the physical characteristics of the wheel to determine rolling resistance of the different tires. The second part (described in this thesis) was to examine the effect of tire type on the user.

Nearly all the work presented in this thesis was done in collaboration with Andrew. Specific contributions by Andrew were: analysis of the data in part one of the experiments, development of the code and algorithm to determine pushrim contact from kinematic data, and the analysis of temporal variables. Additionally, Andrew and I worked collaboratively in the preparation of manuscripts and abstracts related to the study. Working with Andrew was a wonderful experience and I consider him a mentor, a colleague and a friend.

TABLE OF CONTENTS

TABLE OF CONTENTS
(Continued)

TABLE OF CONTENTS
(Continued)

LIST OF TABLES

LIST OF FIGURES

CHAPTER 1

INTRODUCTION

1.1 Objective

The objective of this pilot study was to explore the effect of five commonly used rear wheel tires on: (1) the temporal and spatial characteristics of the push stroke; (2) stroke pattern; and (3) upper limb kinematics during wheelchair propulsion. It was hypothesized that the tires with greater rolling resistance would negatively affect propulsion characteristics as defined by current clinical practice guidelines.

1.2 Upper Limb Pain in Spinal Cord Injured Wheelchair Users

Approximately 1.5 million individuals in the United States use a manual wheelchair for mobility [Kaye 2002]. For these individuals, the ability to stay active in the community and to complete their activities of daily living (ADLs) relies heavily on the function of their upper limbs. Unfortunately, people who use a manual wheelchair over an extended period of time will likely experience upper limb pain. Pain and pathologies of the shoulder and wrist joints are well documented in wheelchair using persons with spinal cord injury (SCI) [Dyson-Hudson 2004].

1.2.1 Impact of Upper Limb Pain on Quality of Life

The presence of upper limb pain in wheelchair using persons with SCI can lead to decreased independence and community integration and an increased risk of secondary conditions such as spasticity, fatigue, obesity, pressure ulcers, and depression [Curtis 1995]. The personal impact of upper limb pain can range from curtailing activities to near

total dependence on others. Dalyan et al. [Dalyan 1999] found that, of individuals experiencing upper limb pain, 26% needed additional help with functional activities and 28% reported limitations of independence due to upper limb pain. Sie et al. [Sie 1992] went so far as to suggest that damage to the upper limbs may be functionally and economically equivalent to a spinal cord injury of higher neurological level.

1.2.2 Wheelchair User's Shoulder

The human shoulder is comprised of the glenohumeral, acromioclavicular, and the sternoclavicular joints connecting the three bones of the shoulder complex (scapula, clavicle and humerus). The complex structure of the shoulder joint allows the greatest range of motion of any joint in the body. This large range of motion comes at the expense of stability under load as is displayed by a similar joint like the hip [Kendall 2005]. The group of tendons and muscles (supraspinatus, infraspinatus, teres minor and subscapularis) collectively known as the rotator cuff, are primarily responsible for stabilization of the shoulder joint. These muscles act to hold the head of the humerus in the glenoid fossa and prevent unwanted translation that could be potentially injurious to the structures of the subacromial space [Kendall 2005]. Unlike the hip, the shoulder is not well designed to undergo the everyday pounding involved in the demands of locomotion [Dyson-Hudson 2004].

1.2.3 Prevalence of Shoulder Pain

A 2004 review of shoulder pain and pathology in wheelchair users by Dyson-Hudson and Kirshblum [Dyson-Hudson 2004] reported the prevalence of shoulder pain in persons with SCI to be between 30% and 78%. Shoulder pain has been primarily associated with

duration of injury, neurological level of injury, and body mass index [Dyson-Hudson 2004].

Studies of the association between the duration of an individual's SCI and shoulder pain have been inconsistent, despite the common belief that prolonged overuse is the primary mechanism of injury [Dyson-Hudson 2004]. Early research on shoulder pain by Nichols et al. and Gellman et al. reported an increased prevalence of shoulder pain with time from injury, the later study reporting 100% prevalence in individuals injured greater than 16 years. [Nichols 1979, Gellman 1988]. More recent studies [Sie 1992, Curtis 1999, Daylan 1999, Noreau 2000] have not found a significant association between the duration of injury and pain. Inconsistent findings about the association of duration of injury and pain may be partially attributed to the effect of age on shoulder pain and the effect of pain on community participation and selection of assistive technology [Curtis 1999]. Increased pain with older age has been reported in the able bodied population [Neer 1977]. Individuals injured for longer periods of time are also likely to be older, making it difficult to differentiate between pain associated specifically with wheelchair use and pain from normal aging. Despite this, in a study of 52 men with paraplegia and 52 age matched individuals Pentland et al. [Pentland 1994] found only duration of injury and not age was associated with pain. Decreased participation in activities which cause pain by individuals with chronic shoulder pain also complicates calculations of the prevalence of shoulder pain. Pain for these individuals may be better assessed by measures of wheelchair use and community participation than measures of symptomatic shoulder pain.

One group that has been identified as having a greater risk for shoulder pain are those individuals injured less than one year [Subbarao 1995, Sie 1992, van Drongelen 2006]. In a 2006 study of individuals with acute SCI (duration of injury <1 year), Van Drogelen et al. reported a higher overall prevalence of pain was associated with higher neurological level of injury, lower upper limb strength, lower functional outcome at 1 year after leaving inpatient rehabilitation [van Drongelen 2006]. Musculoskeletal pain at the beginning of rehabilitation and BMI were strong predictors for pain 1 year after leaving inpatient rehabilitation [van Drongelen 2006].

Neurological level of injury has also been associated with prevalence of shoulder pain in individuals with SCI. Several studies have found individuals with injuries at the cervical level resulting in upper limb impairment (tetraplegia) have a higher prevalence of shoulder pain and earlier onset of shoulder pain than individuals with injuries at the thoracic or lumbar level where upper limb function is spared (paraplegia) [Sie 1992, Curtis 1999, Silfverskiold 1991]. This finding has been attributed to partial innervation of the shoulder and scapular musculature resulting in weakness and decreased stability of the shoulder complex [Silfverskiold 1991, Curtis 1999, Mulroy 2004, Kulig 2001]. Greater pain was found in individuals with high paraplegia than individuals with low paraplegia in a comparative study by Sinnott et al. [Sinnott 2000], implicating limited postural stability due to trunk muscle paralysis may also increase the prevalence of shoulder pain.

Though logically an unhealthy body mass index (BMI) would place greater strain on the upper limb resulting in pain, no study to date has directly linked shoulder pain and BMI in wheelchair using persons with SCI. Boninger et al. found an association between

shoulder radiographic abnormalities from magnetic resonance imaging (MRI) and BMI, but in the same study no strong association was made to pain [Boninger 2001].

1.2.4 Shoulder Pathologies Associated with Propulsion

Musculoskeletal injuries of the shoulder have been cited as the most common cause of shoulder pain in persons with SCI [Dyson-Hudson 2004]. Wheelchair propulsion has been described as an inefficient mode of ambulation [de Groot 2005] that involves repetitive loading of the upper limbs. Previous studies have suggested that the repetitive trauma associated with the magnitude and frequency of this loading is a main cause of shoulder pain and pathology in wheelchair using persons with SCI [Dyson-Hudson 2004, van Drongelen 2005].

The term impingement is often used to describe the mechanical process by which the rotator cuff is impinged by the anterior edge and undersurface of the acromion, the coracoacromial ligament or the acromioclavicular joint [Dyson-Hudson 2004]. Primary impingement is attributed to changes to the structure of the coracoarcromial arch, while the term secondary impingement is used to describe impingement from any factor that leads to a narrowing of the subacromial space. Impingement of the structures of the rotator cuff is thought to be a mechanism in the production of shoulder pain. Elevated forces, fatigue and specific kinematics can each lead to impingement problems [Dyson-Hudson 2004].

During wheelchair propulsion, a vertically oriented force travels up the limb and is directed through the humerus, driving the humeral head into the subacromial joint space. If the passive and dynamic stabilizers of the shoulder cannot control this translation, this motion could result in impingement of the contents of the subacromial

space including the rotator cuff tendons [Dyson-Hudson 2004]. This vertically oriented force increases with increased speed of propulsion, changes in propulsion surface, and incline [Kulig 1998].

Muscle fatigue of the glenohumeral stabilizers can also result in greater superior displacement of the humeral head into the subacromial joint space [Rodgers 1994] causing impingement. Though wheelchair propulsion at self selected speed on flat smooth surfaces has been found to induce only moderate demands on shoulder muscles, prolonged propulsion or propulsion on more demanding terrain can easily result in fatigue [Mulroy 1996]. Placing the shoulder in an internally rotated position, as is commonly found during the push phase of wheelchair propulsion when superior forces on the upper limb are the greatest, can also increase the risk of impingement by placing the greater tuberosity and supraspinatus tendon closer to the acromion [Mulroy 1996].

Overuse is another mechanism contributing to shoulder pain in wheelchair using persons with SCI. Repetitive loading and chronic fatigue of the upper limbs associated with wheelchair population has also been implicated in the development of overuse injuries [Nichols 1979, Bayley 1987, Pentland 1994, Sie 1992]. Due to lower limb paralysis, persons with SCI are forced to rely extensively on their shoulders for mobility and other ADL. The need to perform these activities on a daily basis provides little opportunity for resting of these structures [Dyson-Hudson 2004]. Overuse is defined as repetitive microtrauma that is sufficient to overwhelm a tissue's ability to repair itself [Herring 1987]. Mulroy et al. found the supraspinatus muscle was particularly vulnerable to fatigue and therefore to overuse [Mulroy 1996]. Overuse injuries can reduce the effectiveness of the static stabilizers of the rotator cuff placing a greater demand on the

dynamic stabilizers resulting in greater fatigue of those muscles. Greater fatigue can promote greater overuse and has been associated with glenohumeral joint instability as was discussed earlier.

Radiological studies of the shoulders of wheelchair using persons with SCI most commonly report findings of supraspinatus tendonitis and tear, subacromial bursitis and edema, and thickening of the coracoacromial ligament [Bayley 1987, Escobedo 1997, Boninger 2001, Mercer 2006]. In 33 individuals with paraplegia, Mercer et al. reported individuals who experienced higher posterior, lateral forces, abduction or extension moments at the shoulder were more likely to experience coracoacromial ligament edema or thickening [Mercer 2006]. Increased shoulder internal rotation moment and superior force each made the individual more likely to show pathology on physical exam. Though the etiology of the injuries reported in the radiological studies is well described by the pathomechanics of shoulder injury discussed earlier, there has not been a study definitively linking radiological findings of pathology and the presence of pain.

1.2.5 Wrist Pain and Pathology Associated with Wheelchair Propulsion

Though not as extensively studied as shoulder pain, wrist pain and pathology has also been shown to have a large prevalence in the spinal cord injured wheelchair user population [Boninger 2004]. The human wrist joint is formed by the distal and of the radius and the proximal surface of the bones of the carpus. Movements of the wrist include flexion/extension, radial and ulnar deviation and pronation and supination. Most injuries to the wrist thought to be caused by wheelchair propulsion are associated with carpal tunnel syndrome. The carpal tunnel is the anatomical compartment located at the base of the wrist through which the tendons and nerves responsible for flexion of the

hand pass. The fundamental pathophysiology behind the development of carpal tunnel syndrome is injury to the median nerve [Katz 2002]. Injuries to the median nerve are most commonly associated with numbness or a tingling sensation symptomatic of carpal tunnel syndrome [Katz 2002]. Median nerve damaged has been associated with high-force, high-repetition wrist motions and movements that place the wrist in extreme positions of its normal range of motion [Loslever 1993, Silverstein 1987, Delgrosso 1991, Werner 1998].

Spinal cord injured manual wheelchair users are commonly diagnosed with carpal tunnel syndrome as well as ulnar nerve injury. The incidence of carpal tunnel syndrome in this population ranges from 49% to 63% [Stefaniwsky 1980, Aljure 1985, Gellman 1988, Tun 1988, Davidoff 1991, Burnham 1994, Sie 1992, Boninger 1999, Boninger 2004]. Two studies by Boninger et al. have associated wheelchair propulsion kinetics [Boninger 1999] and kinematics [Boninger 2004] with median and ulnar nerve injuries. Using conduction velocity as a measure of median nerve function Boninger et al. found median nerve damage was associated with increased weight of the user as well as increased cadence, and rate of rise of compressive forces at the wrist during propulsion [Boninger 1999]. A surprising finding of the Boninger et al. study was that a smaller range of motion of the wrist during propulsion was also associated with decreased median nerve function despite previous research indicating greater wrist flexion and extension caused increased pressure in the carpal canal [Boninger 2004]. Boninger et al. suggested the decrease in cadence and forces associated with a larger range of motion was an explanation for this contradiction [Boninger 2004].

1.3 Wheelchair Propulsion Kinematics

1.3.1 Measurment Wheelchair Propulsion Kinematics

Early studies of wheelchair propulsion kinematics utilized digitized film for motion capture allowing joint angles to be captured in a single plane only [Sanderson 1985, Veeger 1989, Veeger 1999, Masse 1992]. These studies established important standards for the temporal and spatial variables associated with the push stroke such as definitions of the push and recovery phases of the stroke pattern, stroke time, push frequency, and contact and release angles [Veeger 1989, Veeger 1991].

In the early 1990's motion capture data acquisition systems became more widely available, enabling much more accurate and efficient three dimensional motion tracking than previously available with video. Building on several descriptions of the shoulder [Browne 1990, An 1991], the first descriptive three dimensional model of wheelchair propulsion biomechanics was developed by Rao et al. in 1996, and utilized passive marker motion capture system to record three dimensional displacement of the upper limbs and trunk [Rao 1996]. The authors described the trunk, upper arm (humerus), forearm and hand as rigid bodies, defined by the motion markers, and labeled each with a right-orthogonal coordinate system describing the orientation of the segment in space. Euler based sequences were then used to rotate the distal segment to the proximal segment in order to define joint angles for the wrist and elbow joints. In the model both the upper arm and the trunk were rotated to the global coordinate frame in order to describe the glenohumeral joint and trunk respectively. Using this model the authors characterized upper limb kinematics as being dominated by humeral elevation and

rotation, and was one of the first authors to comment on the wide intersubject variability in kinematics, especially when compared to gait. [Rao 1996].

The basic methodology described by Rao et al. is still the predominate methodology used today, though modifications have been made by different research groups [Rao 1996]. The most common modifications to the Rao et al. described methodology are variations to the marker set, rigid body coordinate system descriptions, joint center localization techniques and the application of various Euler sequences [Davis 1998, Boninger 1998, Cooper 1999, Newsam 1999, Koontz 2002, Finley 2002, Finley 2004, Feng 2010]. Unfortunately, the differences in kinematic calculations make comparisons between studies difficult.

In 2005, the International Society of Biomechanics (ISB) released a set of recommendations for a standardized calculation of joint motion for the shoulder, elbow, wrist and hand [Wu 2005]. The primary aim of the recommendation was to encourage every author to use the same marker set, local coordinate systems for each segment, and rotation sequence for each joint coordinate system. Briefly, the ISB recommendations for upper limb kinematics suggests an upper limb maker set consisting of the third metacarpoplangeal joint, radial styloid, ulnar styloid, lateral epicondyle, medial epicondyle, acromion, C7 vertebrae, T3 vertebrae, xiphoid process, and sternal notch [Wu 2005]. The upper limb was modeled as three connected rigid body segments to represent the hand, forearm, and upper arm. The distal segment was rotated into the proximal segment (humerus to the trunk) to represent the anatomical angles for the shoulder, elbow, and wrist. A ZXY Cardan rotation sequence was recommended for the

wrist, elbow and trunk. A YXY Euler rotation sequence was suggested for rotation of the humerus to the thorax to define glenohumeral (shoulder) angles.

In response to the ISB recommendation Senk et al. studied the effect of several rotation sequences (YXY, YXZ, ZXY and XZY) on shoulder angles [Senk 2006]. In this study, the ISB recommended sequence of YXY was found to be the sequence most susceptible to gimble lock and lacked accuracy when the movement predominantly occurred between neutral anatomical position and full "backward flexion" (extension) of the humerus [Senk 2006]. Use of one of the three Cardan sequences (YXZ, ZXY, XYZ) were suggested when the movement is dominated by humeral extension past neutral. These authors also suggested that use of one of the Cardan sequences provided greater ease of clinical interpretation considering the resultant joint angle describes flexion/extension, internal/external rotation, and adduction/abduction of the humerus. The ISB recommended YXY sequence describes humeral elevation in two planes relative to the scapula and axial rotation, a definition that lacks clear clinical interpretation [Senk 2006].

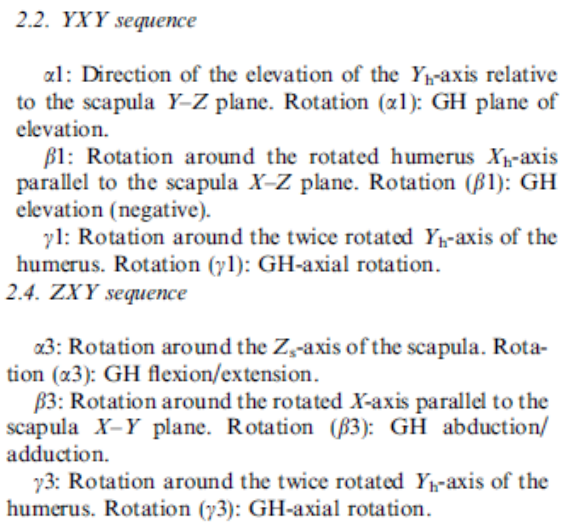

2.2. YXY sequence

α1: Direction of the elevation of the Y_h-axis relative to the scapula Y–Z plane. Rotation (α1): GH plane of elevation.

β1: Rotation around the rotated humerus X_h-axis parallel to the scapula X–Z plane. Rotation (β1): GH elevation (negative).

γ1: Rotation around the twice rotated Y_h-axis of the humerus. Rotation (γ1): GH-axial rotation.

2.4. ZXY sequence

α3: Rotation around the Z_s-axis of the scapula. Rotation (α3): GH flexion/extension.

β3: Rotation around the rotated X-axis parallel to the scapula X–Y plane. Rotation (β3): GH abduction/adduction.

γ3: Rotation around the twice rotated Y_h-axis of the humerus. Rotation (γ3): GH-axial rotation.

Figure 1.1 A comparison of the ISB recommended YXY Euler sequence and a Cardan ZXY alternative offered by Senk et al. [Senk 2006]

Despite the results of Senk et al., Collinger et al. called for a general agreement to use the ISB recommended methodology to bring uniformity to the field of wheelchair propulsion research and allow for greater comparisons amongst different research groups [Senk 2006, Collinger 2008].

Unfortunately, different kinematic calculation methodologies only account for a portion of the large variability in the reported data amongst different groups studying wheelchair propulsion. Variability in individual participant characteristics such as weight, experience, and level of injury limit the ability for comparison between participants. The differences in group characteristics make comparisons between studies challenging. Differences in the experimental set up including the choice to measure ergometer [Mercer 2006], treadmill [Richter 2007] or overground propulsion [Parziale 1991] and the choice of test speed also make comparisons across studies difficult. Studies which utilize a test chair [Newsam 1999, Kulig 2001, Mulroy 2004] generally show greater uniformity in subject kinematic data than studies testing participants in their own chair [Mercer 2006, Collinger 2008] suggesting propulsion biomechanics are associated with wheelchair configuration, and adding another level of complexity to comparisons between individuals and across studies.

1.3.2 Stroke Pattern

The trajectory of the hand during wheelchair propulsion is referred to as stroke pattern and has been the subject of numerous studies [Sanderson 1985, Veeger 1989, Shimada 1998, Boninger 2002, DeGroot 2004, Richter 2007, Aissaoui 2008, Koontz 2009, Kwaciak 2009]. Methodology for studying stroke pattern involves placing a marker on the hand, usually at the site of third metcarpalphalengel joint, and tracking the motion

throughout the stroke cycle. During the push phase of the stroke cycle the hand is forced to follow the arc of the wheel, therefore the greatest differences in stroke patterns are found during the recovery phase [Boninger 2002]. Two early studies of stroke pattern identified two distinct propulsion patterns: circular and pumping [Sanderson 1985, Veeger 1989]. In the circular pattern the hand dropped below the push rim returning to the position at contact and approached pushrim from below and behind in preparation for the following stroke. The pumping pattern was characterized by the hand following the pushrim back and forth on a small arc.

Stroke patterns were further defined by Shimada et al. who identified three patterns of propulsion: semicircular, single looping over propulsion (SLOP), and double looping over propulsion (DLOP) [Shimada 1998]. Boninger et al. added an "arcing" pattern similar to the pumping pattern indentified by Sanderson and Veeger and supplied definitions for the four stroke patterns [Sanderson 1985, Veeger 1989, Boninger 2002]. The four stroke patterns as described by Boninger et al. are [Boninger 2002]:

> "1. Semicircular (SC), recognized by the hands falling below the hand rim during the recovery;
> 2. Single Loop Over Propulsion (SLOP), identified by the hands rising above the hand rim during the recovery phase;
> 3. Double Loop Over Propulsion (DLOP), identified by the hands rising above the hand rim, then crossing over and dropping under the hand rim during the recovery phase;
> 4. Arcing (ARC), recognized when the third MP follows an arc along the path of the pushrim during the recovery phase of the stroke."

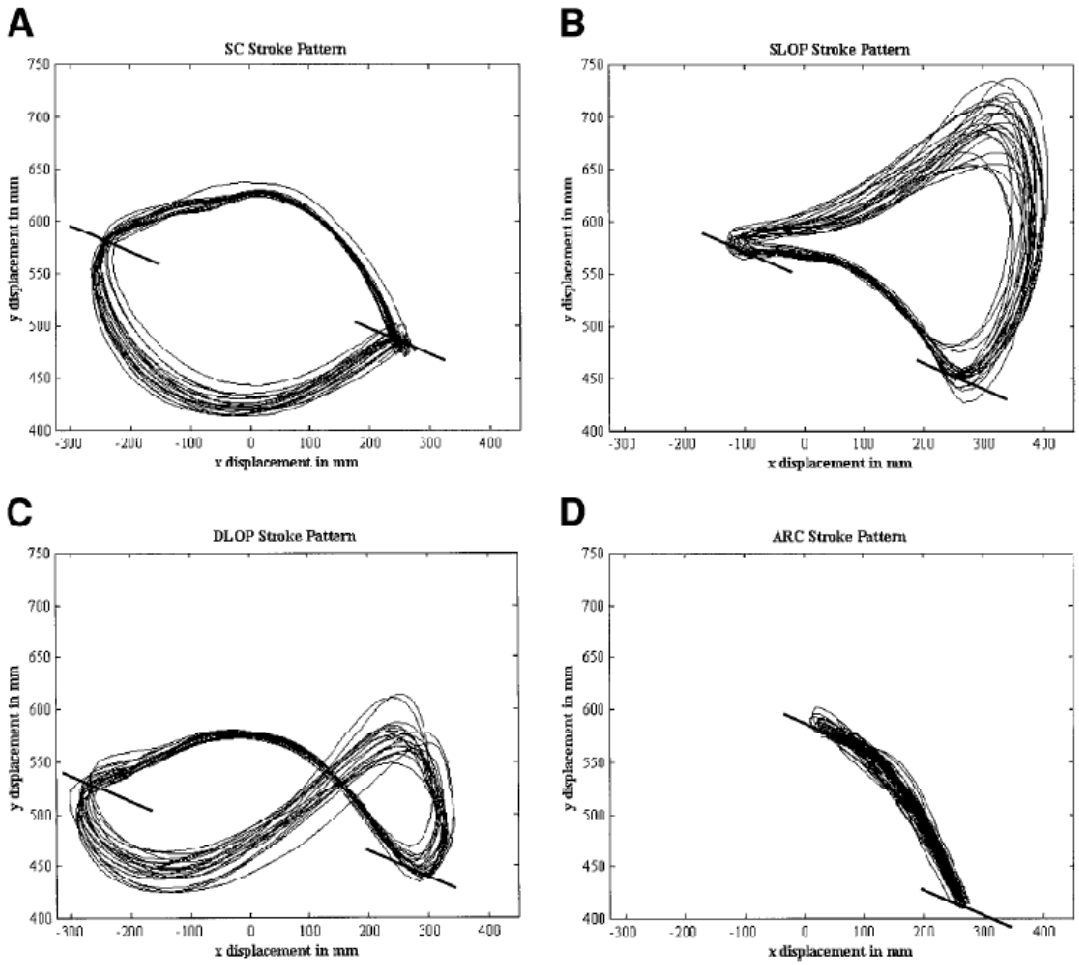

Fig 2. Propulsion patterns. Four classic propulsive strokes are shown: (A) semicircular (SC); (B) SLOP; (C) DLOP; and (D) arcing (ARC). The dark bars to the right of each pattern represent the beginning of the propulsive stroke. The dark bars to the left of each pattern represent the end of the propulsive stroke and the beginning of recovery.

Figure 1.2 Stroke patterns as described by Boninger et al. [Boninger 2002].

Both Veeger et al. and de Groot et al. suggest that the arcing pattern of propulsion is the most mechanically efficient propulsion as defined by the ratio of tangential force to total force exerted on the pushrim [Veeger 1989, de Groot 2004]. In contrast to these findings Boninger et al. found no differences in mechanical efficiency between stroke patterns, and suggested a semicircular pattern may be beneficial to shoulder health [Boninger 2002]. Users with this pattern pushed with a slower cadence and spent more time in the push phase of propulsion reducing the frequency of repetitive loading [Boninger 2002]. Kwarciak et al. reported braking moments at initial contact and release

and concluded that propulsion patterns that approach the wheel from below and behind (SC, DLOP) at initial contact produced significantly smaller braking forces then patterns where the wheel was approached from above (ARC, SLOP) [Kwarciak 2009].

1.4 Factors that Influence Wheelchair Propulsion Biomechanics

Research on wheelchair propulsion biomechanics has predominantly focused on the effects of level of injury [Newsam 1999, Kulig 2001, Mulroy 2004], speed [Koontz 2002, Collinger 2008], and propulsion environment [Kulig 1998, Richter 2007, Cowan 2008, Cowan 2009] on the demand placed on the upper limb.

1.4.1 Level of Injury

Differences have been reported in wheelchair propulsion biomechanics in individuals with SCI at the cervical level resulting in tetraplegia and upper limb impairment, versus those sustaining thoracic injuries resulting in paraplegia where upper limb function is preserved. These differences have been attributed to upper extremity weakness in those with tetraplegia due to selective deinnervation of the upper extremity and trunk muscles resulting in the inability to forcefully extend the elbow, inability to grasp the push rim, and greater trunk instability [Curtis 1999, Dyson-Hudson 2004].

Previous research has shown that individuals with tetraplegia propel at slower speeds, and have higher stroke frequency and shorter stroke cycle time [Newsam 1996, Finley 2004]. Newsam et al. found that wheelchair users with C6 tetraplegic were unable to successfully increase their speed to meet the demands of a fast propulsion condition and questioned the ability of these individuals to community ambulate using a manual wheelchair [Newsam 1996].

A series of papers from a research group at Ranchos Los Amigos Rehabilitation Center focused on the differences in temporal spatial characteristics as well as shoulder kinematics [Newsam 1999], shoulder kinetics [Kulig 2001], and shoulder EMG [Mulroy 2004] during wheelchair propulsion across injury groups ranging from low paraplegia to high tetraplegia. Compared to persons with paraplegia, those with C6 tetraplegia exhibited greater wrist extension [Newsam 1999], as well as larger compressive forces [Kulig 2001] and greater overall EMG activity [Mulroy 2004] at the shoulder.

1.4.2 Speed

Several studies have described the effect of different speeds of propulsion on upper limb kinematics. Early studies concentrating on the push phase of propulsion reported stroke cycle time and push time decreased, while trunk and shoulder flexion as well as power output during push phase increased with increasing speed [Veeger 1989, van der Woude 1989]. Vanlandewijck et al. reported that increased acceleration of trunk and upper limb during the recovery phase, representing increased mechanical work, were associated with increased speed of propulsion, and concluded that propulsion speed affects the movement patterns during recovery [Vanlandewijick 1994]. Increasing propulsion speed from .9 m/s to 1.8 m/s resulted in significant increase in shoulder flexion, abduction and sagittal range of motion in wheelchair users with paraplegia [Koontz 2002, Collinger 2008]. Not surprisingly a great number of studies have shown the close association between greater propulsion speed and an increase in both magnitude of force and rate of loading throughout the upper limb [Boninger 1997, Kulig 2001, Koontz 2002, Mercer 2006, Collinger 2008].

1.4.3 Terrain

Increasing the difficulty of terrain increases the demand on the upper limb and has been shown to influence wheelchair propulsion biomechanics. Previous studies on the effect of incline on propulsion have utilized ramps [Sabick 2004, Koontz 2005, Chow 2009, Koontz 2009, Cowan 2009], inclined treadmills [van der Woude 1988, Veeger 1989, Richter 2007] or applied different resistances to a wheelchair ergometer/dynamometer [Kulig 1998] to simulate incline. Greater incline has been associated with decreases in propulsion velocity [Kulig 1998, Richter 2007, Cowan 2008, Cowan 2009], push angle [Richter 2007, Chow 2009], recovery time [Chow 2009], and increases in push frequency [Koontz 2005, Chow 2009, Cowan 2009] and loads on the upper limb [van der Woude 1988, Veeger 1989, Koontz 2005, Koontz 2009, Cowan 2008, Cowan 2009]. Electromyographic activity of the triceps brachii, antero-middle deltoid, pectoralis major, postero-middle deltoid, extensor carpi radialis and latissimus dorsi increased with greater incline [Chow 2009]. Cowan et al. found that push angle decreased with incline but did not decrease with increased rolling resistance on a flat surface [Cowan 2009]. The authors concluded that during level propulsion, push angle is not affected by surface characteristics. Though studies of kinematics during uphill propulsion are limited, greater forward lean of the trunk has been strongly associated with increased incline [Veeger 1989, Chow 2009]. Incline also may influence an individual's selection of stroke pattern. Several studies report shortening of recovery time often leading to a conversion to an arcing type stroke pattern for uphill propulsion [Richter 2007, Cowan 2009]. Chow et al. concluded the main effect of incline on propulsion mechanics is characterized by increased forward lean and shortening the recovery time [Chow 2009]. It was suggested

that these changes represent strategies to adopt a more compact stroking pattern in order to prevent a significant loss in angular moment of the wheels during recovery [Chow 2009].

Like inclined propulsion, greater surface rolling resistance also increases the demand on the upper limb during wheelchair propulsion. Most wheelchair propulsion testing is done on a flat smooth surface, or either an ergometer or treadmill meant to replicate the demands of propulsion associated with a flat smooth surface. Surfaces with greater rolling resistance such as carpet or grass have been associated with decreased self selected velocity [Newsam 1996, Koontz 2005, Cowan 2008, Cowan 2009], increased push frequency [Koontz 2005, Hurd 2008, Cowan 2009], and greater peak forces [Koontz 2005, Hurd 2008, Cowan 2008, Cowan 2009].

Overall increasing the demand on the upper limb by increasing the difficulty of the terrain has been shown to decrease self selected velocity and was generally accompanied by increased push frequency and little change in stroke cycle time. It appears the main kinematic effect of more demanding propulsion is greater forward lean of the trunk [Cowan 2009].

1.5 Previous Studies of Wheelchair Configuration

To date, studies relating wheelchair propulsion to wheelchair configuration have focused on the effects of rear wheel axle position (also referred to as seat position) [Boninger 2000, Mulroy 2005], and the effects of wheelchair weight [Parziale 1991, Beekman 1999].

Studies have shown that the vertical and horizontal position of the rear axle has a significant influence on wheelchair propulsion biomechanics. A 1986 study by Brubaker et al. suggested a more anterior axle position decreases wheelchair rolling resistance, resulting in increased propulsion efficiency [Brubaker 1986]. This increased efficiency has been demonstrated in kinematic [Hughes 1992; Boninger 2000], kinetic [Boninger 2000, Mulroy 2005] and electromyographic measurements [Masse 1992, Guitierrez 2005] of wheelchair propulsion biomechanics. A more anterior axle position has been associated with increased pushrim contact angle [Hugh 1992; Boninger 2000] and decreased push frequency [Boninger 2000], decreased magnitude [Cowan 2009] and rate of pushrim loading [Boninger 2000], and decreased superior shoulder joint force [Mulroy 2005]. Guitierrez et al. found no changes in shoulder muscle timing and intensity for free propulsion, but reduced intensity of the pectoralis major and anterior deltoid were found for the more posterior axle position in ramp and fast propulsion conditions [Guitierrez 2005].

A higher vertical axle, resulting in a smaller shoulder to hub distance, has been shown to reduce oxygen consumption [van der Woude 1989], reduce muscle activity [Masse 1992], increase upper limb range of motion [van der Woude 1989, Hughes 1992], and increase push angle [van der Woude 1989, Boninger 2000, Kotajarvi 2004, Richter 2001]. Raising the vertical axle position has also been associated with decreased push frequency [Boninger 2000, Richter 2001], decreased rate of rise of pushrim force [Boninger 2000], decreased shoulder torque [Richter 2001], and increased elbow extension torque [Richter 2001]. Biomechanical benefits associated with a smaller

shoulder to axle distance are often attributed to greater access to the pushrim [van der Woude 1989, Boninger 2000].

Numerous studies of energy expenditure have found lighter wheelchairs improve performance compared to standard wheelchairs [Hilbers 1987, Parziale 1991, Beekman 1999], yet the association between wheelchair weight and propulsion mechanics is not as strong. Bednarczyk et al. reported the addition of 10kg weight did not affect propulsion kinetics of adults and children with spinal cord injury across tiled floors [Bednarczyk 1994]. The only existing study of wheelchair weight on propulsion kinetics is the study by Cowan et al. in able-bodied older adults [Cowan 2009]. Cowan et al. reported a decrease in self selected velocity and increase in push rim forces with increased wheelchair weight [Cowan 2009].

1.6 Guidleines for Healthy Propulsion

In 2005, the Paralyzed Veterans of America Consortium for Spinal Cord Medicine (PVA-ACSCM) reviewed findings from studies of wheelchair biomechanics, and ergonomics, pathology, and exercise to create a clinical practice guideline for health care professionals to preserve upper limb function after spinal cord injury [PVA 2005]. Created by a consortium of clinicians and researchers, the clinical practice guidelines present a series of recommendations intended to reduce the strain on the upper limb during activities of daily living [PVA 2005]. Recommendations regarding assessment, ergonomics, wheelchair selection and setup, wheelchair training, environmental adaptations, exercise, and pain management are included. Ergonomic recommendations relating to wheelchair propulsion include: 1) minimize the frequency of repetitive upper limb tasks; 2) minimize

the force required to complete upper limb tasks; 3) avoid extreme positions of the wrist including wrist extension when loaded; and 4) avoid potentially injurious or extreme positions at the shoulder, including extreme internal rotation and abduction [PVA 2005]. In order to encourage healthier propulsion mechanics the guidelines recommend the rear axle be placed as far forward as possible without compromising stability, and at a height that when the hand is on the top dead-center of the pushrim, the angle between the upper arm and the forearm is between 100 and 120 degrees. In addition, wheelchair users should use the lightest weight adjustable wheelchair possible. With regards to stroke pattern the guidelines encourage participants to use a long smooth push stroke in order to minimize propulsion frequency and the rate of loading on the upper limb.

Cowan et al. proposed a method for clinicians to objectively evaluate manual wheelchair propulsion using a commercially available instrumented push rim [Cowan 2000]. The need for intervention was based on the need to increase speed, reduce push frequency and reduce the forces associated with propulsion. Suggested interventions include combinations of strength training, propulsion training, and alterations in the individual's current chair set-up, or use of a lighter weight, more adjustable chair [Cowan 2008].

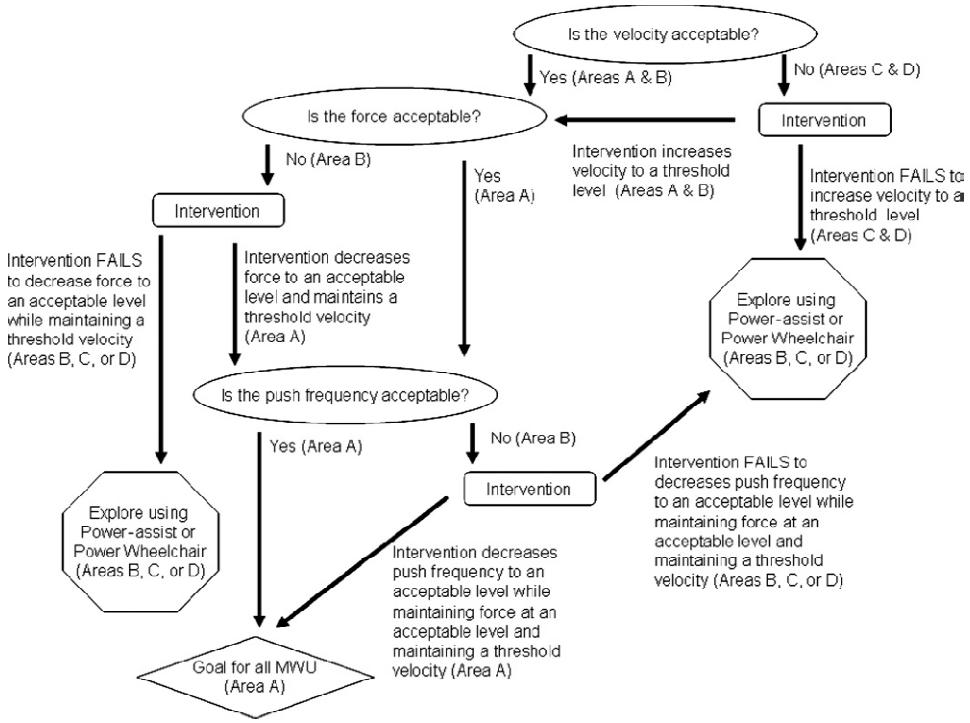

Figure 1.3 A flow chart detailing suggested clinical interventions for wheelchair users with shoulder pain [Cowan 2008].

One important and easily managed aspect of wheelchair use that is not addressed by the guideline [PVA 2005] or Cowan et al. [Cowan 2008] is the rear wheel tires. Changing rear wheel tire type does not require significant costs, effort, or lifestyle changes. Before a recommendation on tires can be proposed, research is needed to determine the impact of tire selection on wheelchair propulsion and upper limb strain.

1.7 Wheelchair Rear Tires

Rear wheel tires contribute to the rolling resistance of the wheelchair. The main cause of rear wheel tire rolling resistance is inelastic deformation of the tire as it rolls across a surface [Kauzlarich 1985]. Factors such as tire design and material composition, laden weight, and the interaction between the tire and the surface all determine the magnitude of deformation. Several studies [Kwarciak 2009, Kauzlarich 1985; Gordon 1989;

Sawatzky 2004] have investigated the rolling resistance of wheelchair tires and how they affect wheelchair and user performance. Throughout these studies, it has been shown that pneumatic tires have less rolling resistance than solid airless tires and are less affected by increased loading on the wheelchair. This allows a wheelchair equipped with pneumatic tires to roll farther than wheelchair equipped with solid tires for the same applied energy [Kwarciak 2009, Sawatzky 2004]. Even under sub-optimal inflation pressures (as low as 50% of the recommended pressure), pneumatic tires have been shown to roll farther than solid tires [Sawatzky 2004].

Although pneumatic tires offer a clear advantage in terms of rolling resistance, wheelchair users may prefer solid tires because they require relatively no maintenance and have no risk of puncture or becoming flat. For these individuals, the benefits of a lower maintenance tire may outweigh the perceived benefit of a tire with lower rolling resistance. This is a reasonable conclusion, given the lack of research linking wheelchair tires to wheelchair function and use. One key piece of information that is missing from the decision making process is how tires influence the demands placed on the user. With growing efforts to preserve upper limb health of manual wheelchair users, and thus independence, clinicians, users, and researchers must understand how individuals respond to different tires and how the resulting biomechanics may affect risk of upper limb injury.

CHAPTER 2

PRELIMINARY STUDIES

2.1 Rolling Resistance on Commonly Used Wheelchair Tires

This thesis is presented as the second part of a two part study. Part one of the study, published by Kwarciak et al. [Kwarciak 2009], reported on the rolling resistance and coast-down distance of two pneumatic tires, two airless solid tires, and a pneumatic tire with a solid fill. All tires were attached to similar rear wheels and fitted to a standard rigid-frame wheelchair (Quickie GPV, Sunrise Medical, Longmont, CO; weight: 9 kg, rear wheel camber: 3.5 degrees). The wheelchair was secured over a two-drum dynamometer. The right wheel was accelerated up to a speed of at least 2 m/s, acceleration was discontinued and the resultant deceleration was measured and reported as coast down time. Wheel rotations were recorded with a 7-camera Vicon motion capture system and spherical reflective markers were placed on the axle and pushrim of each wheel. Three sets of weights (45.4 kg, 68.0 kg, and 90.7 kg) were added to the seat of the wheelchair to simulate different users. Ten trials were collected for each tire and each weight condition for a total of 150 trials. The marker trajectories measured during each trial were used to determine the deceleration of the wheel (a_d) between 2 m/s and 1 m/s. Experimental data on the deceleration of the wheel with each tire permitted the calculation of rolling resistance (F_{RR}) using a simplified model of wheelchair propulsion on an inertial roller system (Equation 2.1) presented by Cooper et al. [Cooper, 1990].

$$F_{RR} = -a_d/R^2*(I_w + 5.47R) \quad (2.1)$$

In equation 2.1, R is the radius of the wheel and I_w is the moment of inertia of the wheel. In addition to rolling resistance, coast-down distance, or the linear distance traveled by each wheel between 2 m/s and a complete stop were also determined. The calculations of coast-down distance were performed in order to compare results with those of Sawatzky et al. [Sawatzky 2004]. To better approximate the testing conditions of the Sawatzky et al. study, the lower speed threshold was set to zero. Assuming a constant deceleration, coast-down distance (CDD) was computed using the equation of motion:

$$CDD = 0.5*a_d t^2 + v_o t \quad (2.2)$$

where v_o is the initial velocity (approximately 2 m/s) and t is the coast-down time ($t = v_o/a_d$).

These calculations confirmed the findings of previous studies [Gordon 1989, Sawatzky 2004] that pneumatic tires have a lower rolling resistance and roll farther than solid tires. Table 2.1 shows a summary of the findings in Kwarciak et al. Weight conditions refer to the total amount of weight on the right rear wheel. Given the differences in specific tires and testing conditions, rolling resistances are similar to those reported by Gordon et al. [Gordon 1989] and differences in coast-down distances, between the PV, PO and KIK tires, are comparable to those reported by Sawatzky et al. [Sawatzky 2004].

Table 2.1 Mean Rolling Resistance and Coast-down Distance for each Tire Under each Weight Condition

	223.6 N		291.3 N		337.6 N	
Tire	F_{RR} (N)	CDD (m)	F_{RR} (N)	CDD (m)	F_{RR} (N)	CDD (m)
PV	1.678	22.83	2.079	18.48	2.617	14.65
PO	1.857	20.14	2.340	15.99	2.881	13.02
KIK	3.113	12.50	4.521	8.65	5.876	6.67
CSSI	3.551	10.92	5.195	7.43	7.311	5.28
AL	3.908	9.89	6.202	6.22	8.550	4.54

PV = Primo V-Trak (100 pounds per square inch [psi] pneumatic); PO = Primo Orion (75 psi pneumatic); KIK = KIK Mako (solid), CSSI = Cheng Shin tire with solid insert, AL = Alshin (solid); N = Newtons;
m = meters

Beyond the findings of previous studies, Kwarciak et al. was able to demonstrate the distinct differences between common wheelchair tires both within and across weight conditions. Not only did the pneumatic tires roll easier and farther than the solid tires, they were less affected by the increases in weight. This is an important point for clinicians and manual wheelchair users to consider when selecting a tire. The weight of the wheelchair and the user will affect rolling performance and should factor into the decision making process. Selecting a solid tire for a heavier individual, or someone with a heavy wheelchair, could exacerbate the forces and moments on the joints during propulsion and increase the risk of upper limb injury. This information is also important for researchers who wish to record propulsion mechanics. In order to properly represent each person's typical biomechanics, the testing setup, including tires, should be representative of each person's typical equipment.

CHAPTER 3

EXPERIMENTAL SET-UP AND ANALYSIS

3.1 Inclusion and Exclusion Criteria

To be included in the study, individuals were required to be between 18 and 65 years of age, have a spinal cord injury between the C5-L5 vertebrae, be at least one year post injury, and use a manual wheelchair at least 40 hours per week. Exclusion criteria included upper limb injury within the previous year, pain as a result of a syrinx or complex regional pain syndrome, or pregnancy. The study physician screened each participant to ensure that he/she was not at risk of serious injury. Institutional Review Board approval was obtained from the Kessler Foundation Research Center. Informed consent was obtained from participants prior to participating in the study. Table 3.1 lists the key characteristics for each participant.

Table 3.1 Participant Characteristics

Participant	Level of Injury	Age (yrs)	Weight (kg)	Duration of injury (yrs)
P1	T6	24	67.59	6
P2	T6	29	63.96	5
P3	T10	31	71.67	3.5
P4	T3	47	88.45	3.5
T1	C6	34	70.76	15
T2	C6/C7	26	102.06	7
T3	C6/C7	46	106.60	16
T4	C6/C7	41	81.65	15
Paras	-	32.8 ± 9.9	72.9 ± 10.8	4.5 ± 1.2
Tetras	-	36.8 ± 8.7	90.3 ± 16.9	13.25 ± 4.2
All	-	34.8 ± 8.9	81.6 ± 16.1	8.9 ± 5.5

3.2 Tire Selection

Five different tires were selected for testing including four tires commonly used by manual wheelchair users [Kwarciak 2009]. The fifth tire selected was the solid tire provided with a commercially-available instrumented wheelchair wheel (SmartWheel, Three Rivers Holdings, LLC, Mesa, AZ). The five tires were: (1) Primo V-Trak pneumatic tires (Gallop Cycle Corp., Long Beach, CA); (2) Primo Orion pneumatic tires; (3) KIK Mako solid tires (Amerityre Corp., Boulder City, NV); (4) Cheng Shin pneumatic tires (Cheng Shin Rubber Ind. Co., Ltd., Xiamen, China) with solid inserts; and (5) Alshin solid tires (Alshin Tire Corporation, Rancho Cucamonga, CA). Each set of tires was mounted on a pair of 0.61 m Sunrims SW600 wheels with radial spokes (Hayes Bicycle Group, Mequon, WI). The Primo V-Trak and the Primo Orion were inflated to the recommended pressure of 100 psi and 75 psi, respectively. Table 3.2 lists the type, profile, and rolling resistance force (Frr) of each tire. Additional physical characteristics for the tires used in this study are described elsewhere [Kwarciak 2009].

Figure 3.1 Selected tires used for experimentation.

Table 3.2 Tire Characteristics

Tire	Type	Profile	Frr at 150 lbs Loading (N)*	Frr at 200 lbs Loading (N)*
Primo V-Trak (PVT)	Pneumatic	Low	2.1	2.6
Primo Orion (PO)	Pneumatic	Full	2.3	2.9
KIK Mako (KM)	Solid	Low	4.5	5.9
Cheng Shin (CSSI)	Solid insert	Full	5.2	7.3
Alshin (AL)	Solid	Full	6.2	8.6

* Frr at different loads obtained from Kwarciak et al.

3.3 Experimental Setup

Participants were tested in their own wheelchairs, which were secured to a platform positioned over a custom-built roller system. Time was allowed for acclimation to pushing on the rollers prior to testing. Participants were asked to push at a self-selected speed, as if they were pushing down a hallway. Participants verbally indicated when they had reached a steady-state self-selected speed, at which point data were collected for 20 seconds. During each trial, participants were asked to rate their perceived exertion using the Borg scale [Borg 1988].

Figure 3.2 Experimental setup.

3.4 Kinematic Data Collection and Analysis

Three-dimensional kinematic data were collected at 120 Hz using a passive marker motion capture system (Vicon, Oxford, UK). Reflective markers were placed on each wheel (hub and spoke) and on the bony landmarks of the upper limbs and trunk in accordance with the ISB recommendations [Wu 2005]. Kinematic data were filtered using a 4th order, zero phase, low-pass Butterworth filter with a 7-Hz cutoff frequency [Sanderson 1985]. The upper limb was modeled as three connected rigid body segments to represent the hand, forearm, and upper arm. Each segment was described using the ISB-recommended local coordinate system [Wu 2005]. The distal segment was rotated into the proximal segment (humerus to the trunk) using a Cardan ZXY order rotation sequence to represent the anatomical angles for the shoulder, elbow, and wrist. The trunk

was rotated into the laboratory global reference frame [Wu 2005] also using a ZXY rotation. ISB recommended rotations were used at all joints except the shoulder. A Cardan sequence (ZXY) was chosen for shoulder instead of the ISB recommended Euler sequence (YXY). This decision was based off of recommendations by Senk et al. for the selection of a Cardan rotation sequence when the shoulder motion is dominated by humeral extension beyond anatomical neutral position and to give greater similarity to the clinically defined planes of movement [Senk 2006].

Seven motions of the trunk and upper limb were analyzed including: trunk flexion-extension, shoulder flexion-extension, shoulder abduction-adduction, shoulder internal-external rotation, elbow flexion-extension, wrist flexion-extension and wrist ulnar and radial deviation. All joint angles were referenced to zero at a defined neutral seated position with the participant's arms placed at their sides with the forearms at 90 degrees to the humerus, palms facing medially, and fingers pointing forward. Maximum joint angles and range of motion during the push phase were selected for outcome variables. The joints of the upper extremity are at the greatest risk for impingement at the extremes of their range of motion during loading [PVA 2005]. All joint angles were presented as mean (± 1 standard deviation) over five consecutive strokes.

3.5 Data Processing

All kinematic data was normalized to 100% of the stroke cycle. The stroke cycle, the contact phase, and the recovery phase [Sanderson 1985, Kwarciak 2009] were identified using the third metacarpal-phalangeal joint (hand) and the hub marker trajectories. Typically, phases are identified using pushrim forces and moments [Kwarciak 2009],

however no such data were available in this study. Instead, the limits of the contact phase were identified as the first and last points at which the hand was moving forward and with a positive (forward-directed) angular velocity about the hub marker. To refine the estimate of pushrim release, the contact phase was trimmed to the last point at which the hand maintained a downward path. The recovery phase was the period between consecutive contact phases. From these phases, the length of the pushrim contact (in seconds) and the percentage of the stroke cycle dedicated to pushrim contact (contact phase time divided by the total stroke cycle time) was determined.

Markers on the wheel and hand were also used to determine wheel speed, push frequency, contact phase angle, and the angles at which the hand contacted and released the pushrim. Wheel speed (m/s) was computed as the rate at which the marker on the spokes revolved around the hub marker, multiplied by the radius of the wheel. Push frequency (strokes/m) was calculated as the reciprocal of the average distance traveled by the wheel during each of the selected strokes. This representation of push frequency was used, as opposed to the traditional measure of strokes per second, to account for differences in wheel speed and to provide a more functional description of the push. All calculations of wheel angle were relative to the orientation of the vector joining the hub marker to the hand marker. The contact angle and the release angle were the angles between the hub to hand vector and the horizontal axis at initial contact and release, respectively. The contact phase angle, defined as the angle through which the hand rotates while in contact with the pushrim, was the difference between the pushrim release angle and the pushrim contact angle. The percentage of the stroke cycle spent in the

contact phase was also identified as a main outcome variable. All outcome variables were computed as the mean (± 1 standard deviation) over five consecutive strokes.

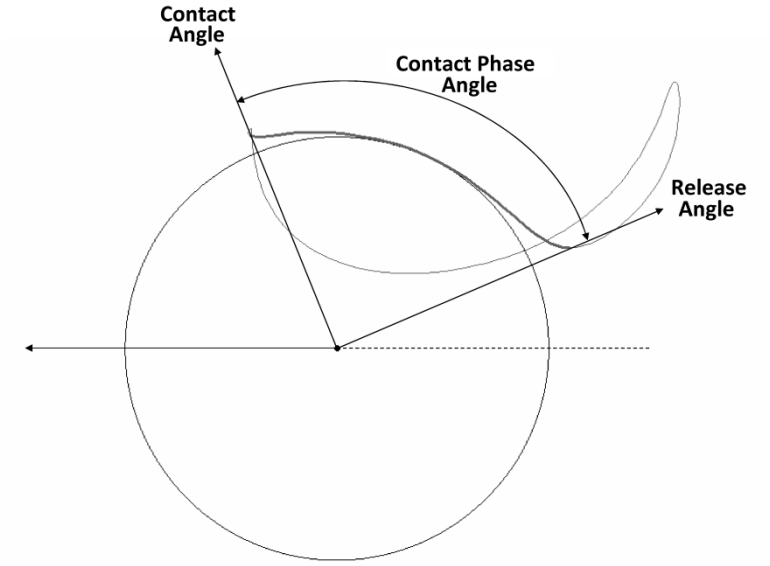

Figure 3.3 Definition of spatial variables.

To examine stroke technique, three independent reviewers examined the sagittal plane hand marker trajectories and described each using one of four patterns [Boninger 2002, Kwarciak 2009]: arcing (ARC), single-looping over propulsion (SLOP), double-looping over propulsion (DLOP), and semi-circular (SC). To further examine the effect of different tires on stroke technique, the total distance covered by the hand in the sagittal plane was calculated. This distance was used to quantify changes within similar stroke patterns. All calculations and examinations of propulsion data were performed with custom routines built in Matlab (The MathWorks, Inc., Natick, MA).

One-way ANOVAs were used to determine if tire had a significant impact on each of the temporal-spatial variables and perceived exertion. Post-hoc analyses, with a Bonferroni adjustment, were used to compare variables across tires for all participants and for each group (paraplegia and tetraplegia). Statistical analyses were performed using SPSS 16.0 software (SPSS Inc., Chicago, IL) with significance set to $P < 0.05$.

CHAPTER 4

RESULTS

4.1 Participants

Participants (7 male, 1 female) were subdivided into individuals with paraplegia (Paras) and individuals with tetraplegia (Tetras) based on level of injury. All participants with tetraplegia had upper limb impairment. Outcome measures were averaged for each injury group and for the entire study population. All results are presented in order of increasing tire rolling resistance.

4.2 Temporal Variables

Figure 4.2 shows the mean temporal variables for each injury group for each tire. All participants achieved the greatest self-selected speed with the PVT tire (1.42 ± .36 m/s) and the slowest self-selected speed with the AL tire (1.06 ± .17 m/s). As tire rolling resistance increased, self-selected wheel speed decreased (Figure 4.2A), with the exception of the KM tire, which the paraplegia group pushed .04 m/s faster than the PO tire. In response to increased rear wheel tire rolling resistance, users increased push frequency (Figure 4.2B). The largest increase in push frequency was experienced between the KM and CSSI tires (28 ± 26%). Between the injury groups, the paraplegia group used less pushes per meter than the tetraplegia group across all tires. Stroke cycle length (Figure 4.2C) trended towards quicker strokes with increased rolling resistance; however, the trend was not consistent across tires within either group. Participants spent

a greater percentage of the stroke cycle in the contact phase as rolling resistance increased, except for a drop in contact phase time for the paraplegia group with KM tire (Figure 4.2D).

One-way ANOVAs revealed a significant ($p < .05$) effect of tire on the push frequency and wheel speed of all participants, and on the contact phase and wheel speed of the paraplegia group. Although most individual tire comparisons were not significant, the wheel speed of the paraplegia group, with the PVT tire, was significantly ($p = .012$) faster than the wheel speed with the CSSI and AL tires.

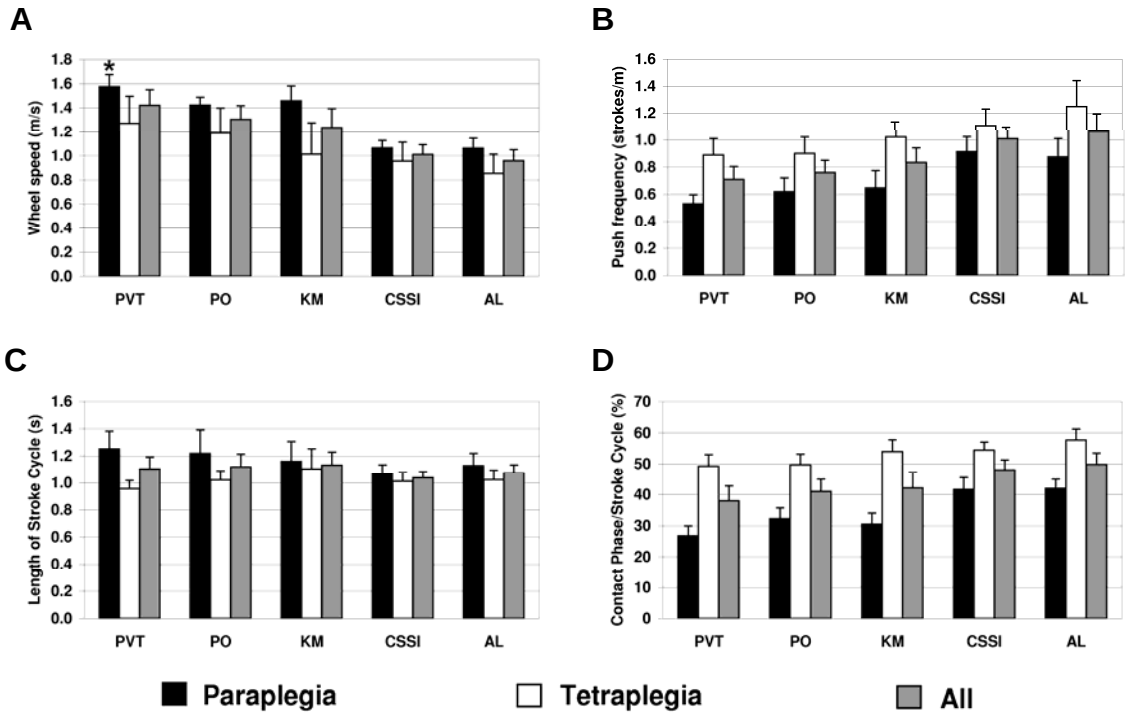

Figure 4.2 Temporal variables: (A) wheel speed; (B) push frequency; (C) length of stroke cycle; and (D) percentage of stroke dedicated to the contact phase. *Significantly ($p = .012$) faster than wheel speed with CSSI and AL.

There was no trend in the contact, release or phase angles with increased rolling resistance. A one-way ANOVA revealed no significance in spatial parameters across the tires.

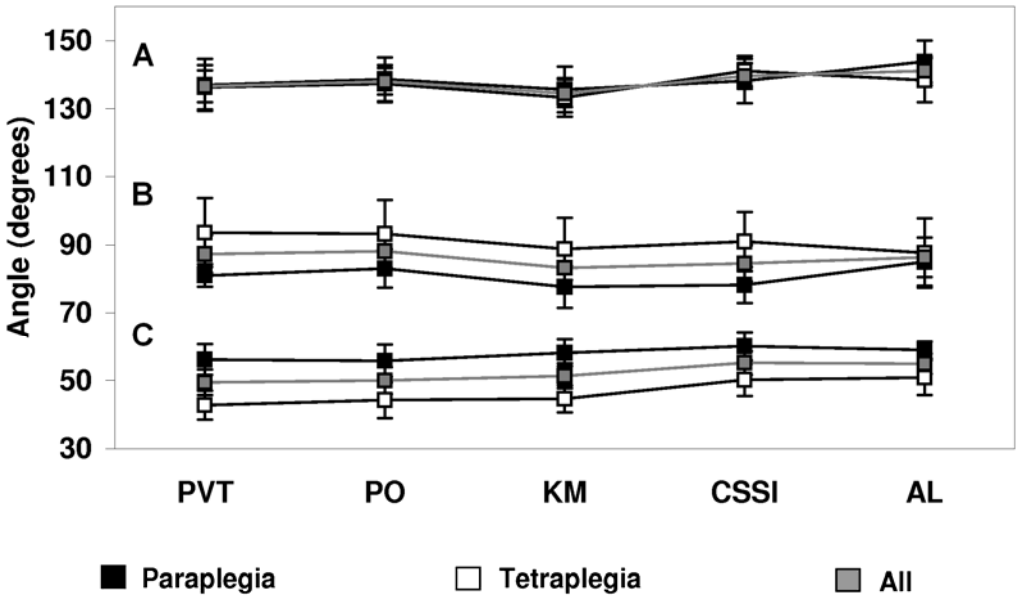

Figure 4.2 Spatial variables across all five tire types: (A) Release Angles; (B) Contact Phase Angles; and (C) Contact Angles.

4.3 Perceived Exertion

Figure 4.3 shows the mean Borg ratings of perceived exertion (RPE) for each tire. There was little change between the RPE of either the paraplegia group or the tetraplegia group for the PVT, PO, and KM tires; however, the ratings statically increased for the CSSI and AL tires. On average, all participants experienced a 4.13 point (55%) increase in perceived exertion between the PVT and both the CSSI and AL tires.

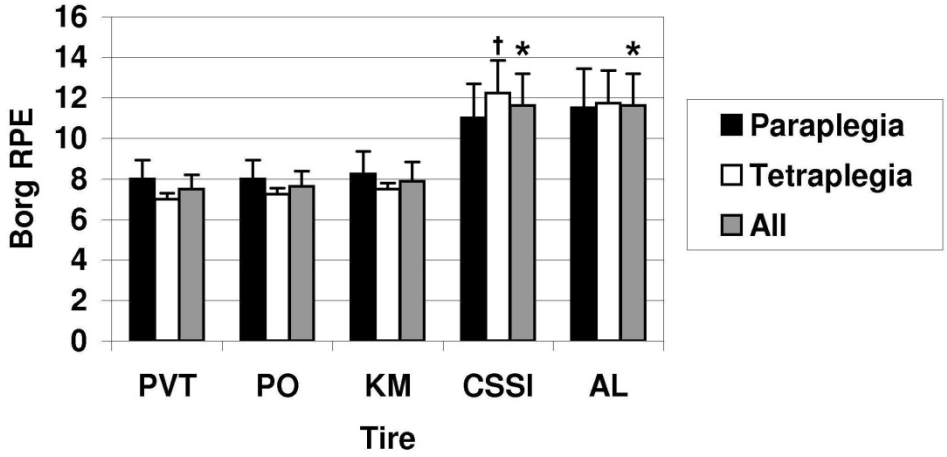

Figure 4.3 Mean Borg ratings of perceived exertion for each tire. *Significantly ($p < .03$) higher than PVT, PO, and KM RPE. †Significantly ($p = .035$) higher than PVT RPE.

4.4 Stroke Pattern

Three participants from the paraplegia group showed a change in stroke pattern from a looping propulsion pattern (SLOP or DLOP) when using the tires with lower rolling resistance (PVT, PO, KM), to an arcing propulsion pattern when using tires with greater rolling resistance (CSSI, AL). Though the remaining participants showed no change in stroke pattern, all participants tended to restrict total hand movement throughout the stroke (PVT = 1.05 ± 0.19m; PO = .97 ± 0.15m; KT = 1.00 ± 0.20m; CSSI = .91 ± 0.12m; AL = .90± 0.16m) in response to increased rolling resistance. Figure 4.4 shows the sagittal plane hand marker trajectories of two participants: one who had a distinct change in stroke pattern (P1), and one who exhibited no change in pattern type, but a reduction in the distance traveled by the hand throughout the stroke (T4).

Table 4.1 Stroke Patterns of each Participant with each Tire

	Paraplegia				Tetraplegia			
Tire	P1	P2	P3	P4	T1	T2	T3	T4
PVT	DLOP	SLOP	DLOP	SLOP	ARC	DLOP	SC	DLOP
PO	SLOP	SLOP	DLOP	SLOP	ARC	SC	SC	DLOP
KM	ARC	SLOP	DLOP	SLOP	ARC	DLOP	SC	DLOP
CSSI	SLOP	SLOP	ARC	ARC	ARC	DLOP	DLOP	DLOP
AL	ARC	SLOP	ARC	ARC	ARC	DLOP	SC	DLOP

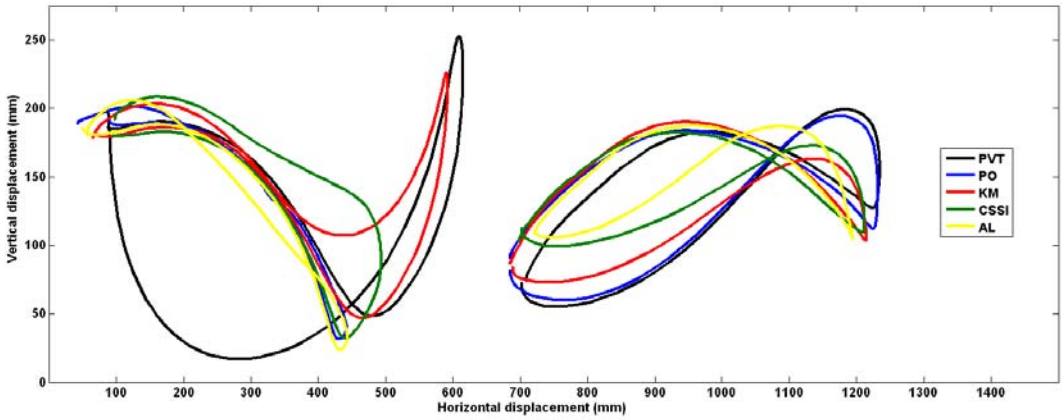

Figure 4.4 Stroke patterns of participant P1 (left) and T4 (right) for each tire.

4.5 Kinematics

Sagittal Plane Trunk Kinematics

Sagittal plane trunk kinematics were characterized by a short period of trunk flexion following initial pushrim contact, then trunk extension throughout the rest of the contact phase. A return to flexion was seen during the recovery phase, in preparation for the following stroke. With increased rolling resistance, mean trunk position became increasingly flexed, and sagittal plane trunk range of motion increased (Table 4.4). Across all tires, the tetraplegia group had a greater mean range of motion (10.18 ± 1.97°) than the paraplegia group (7.16 ± .68°).

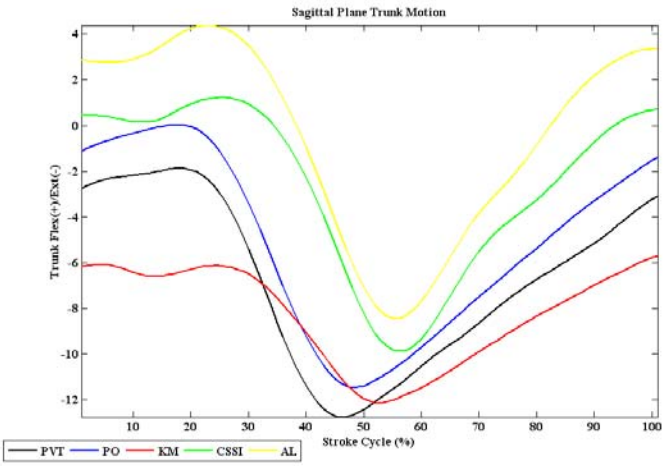

Figure 4.5 Sagittal plane trunk motion of participant T2 for each tire.

Table 4.2 Mean Sagittal Trunk Position and Range of Motion (degree) for each Tire

Variable	Group	PVT	PO	KM	CSSI	AL
Mean Trunk Position	Para	-3.25 ± 6.48	-0.60 ± 7.80	-3.30 ± 7.17	-2.33 ± 7.87	-0.99 ± 7.30
	Tetra	0.83 ± 5.77	1.12 ± 5.12	0.41 ± 6.58	4.78 ± 6.92	5.21 ± 6.98
	All	-1.21 ± 6.09	0.26 ± 6.18	-1.44 ± 6.67	1.22 ± 7.84	2.11 ± 7.40
Range of motion	Para	6.00 ± 3.98	7.31 ± 4.02	7.75 ± 4.35	7.42 ± 5.05	7.33 ± 3.69
	Tetra	9.16 ± 3.28	10.57 ± 1.27	7.65 ± 3.44	12.95 ± 3.67	10.60 ± 3.21
	All	7.58 ± 3.78	8.94 ± 3.27	7.70 ± 3.63	10.18 ± 5.04	8.96 ± 3.65

Shoulder Kinematics

Three-dimensional angles at the shoulder were characterized by a position of maximal extension, minimal abduction, and minimal internal rotation at contact for all tires. Throughout push phase, internal rotation and abduction increased as the arm moved towards shoulder flexion. Decreased shoulder abduction and internal rotation accompanied shoulder extension during recovery phase as the arm returned to the position at initial contact. Table 4.5 displays selected shoulder angles during push phase in the three planes of motion for each tire. Maximum shoulder abduction appears

unaffected by tires with higher rolling resistance in both individuals with paraplegia and tetraplegia. Between the PVT and AL tires, maximum shoulder internal rotation angle increased 9.56 ± 7.49° for the tetraplegia group and 7.09 ± 3.20° for the paraplegia group. In the sagittal plane, both groups showed an increase in shoulder range of motion as tire rolling resistance increased, resulting from an increase in the peak flexion angle.

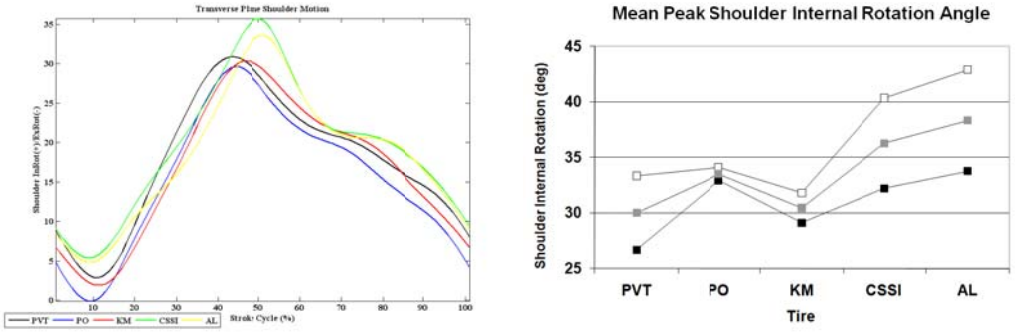

Figure 4.6 Coronal plane trunk shoulder of participant T4 for each tire.

Table 4.3 Tri-planar shoulder angles (degrees) for each Tire

Variable	Group	PVT	PO	KM	CSSI	AL
Maximum Abduction	Para	26.08 ± 6.61	28.91 ± 7.92	25.72 ± 8.15	28.45 ± 6.79	29.42 ± 7.82
	Tetra	25.39 ± 11.86	26.19 ± 11.50	25.84 ± 11.11	29.18 ± 12.23	28.70 ± 13.16
	All	25.74 ± 8.89	27.55 ± 9.26	25.78 ± 9.02	28.81 ± 9.17	29.06 ± 10.03
Maximum Internal Rotation	Para	26.68 ± 9.88	32.93 ± 8.54	29.11 ± 10.51	32.21 ± 10.86	33.77 ± 10.37
	Tetra	33.35 ± 15.13	34.11 ± 16.71	31.80 ± 18.13	40.35 ± 15.45	42.91 ± 20.16
	All	30.01 ± 12.35	33.52 ± 12.30	30.46 ± 13.79	36.28 ± 13.11	38.34 ± 15.62
Maximum Flexion	Para	-8.28 ± 16.54	0.12 ± 3.68	0.98 ± 9.25	-1.39 ± 13.81	1.25 ± 9.98
	Tetra	-6.07 ± 10.27	-4.28 ± 11.22	-6.17 ± 10.91	-0.56 ± 9.65	-0.70 ± 11.41
	All	-7.18 ± 12.80	-2.08 ± 8.08	-2.60 ± 10.12	-0.98 ± 11.04	0.27 ± 9.98
Maximum Extension	Para	47.09 ± 6.59	44.36 ± 6.52	45.76 ± 7.07	43.72 ± 7.31	45.12 ± 7.09
	Tetra	42.10 ± 5.20	42.26 ± 4.65	42.23 ± 6.76	38.95 ± 7.56	39.73 ± 7.52
	All	44.59 ± 6.11	43.31 ± 5.36	43.99 ± 6.68	41.33 ± 7.34	42.43 ± 7.36

Elbow Sagittal Plane Kinematics

Sagittal plane elbow motion was characterized by an initial flexing of the elbow followed by extension. At no point in the stroke cycle did the elbow reach less than 90° anatomical. Between the PVT and AL tires, the paraplegia group increased peak elbow extension during the contact phase (7.27 ± 5.58°), while the tetraplegia group exhibited a much smaller increase (0.49 ± 5.07°). Minimum elbow extension showed little change for both groups, resulting in an increased range of motion in the paraplegia group with increased tire rolling resistance (Table 4.5).

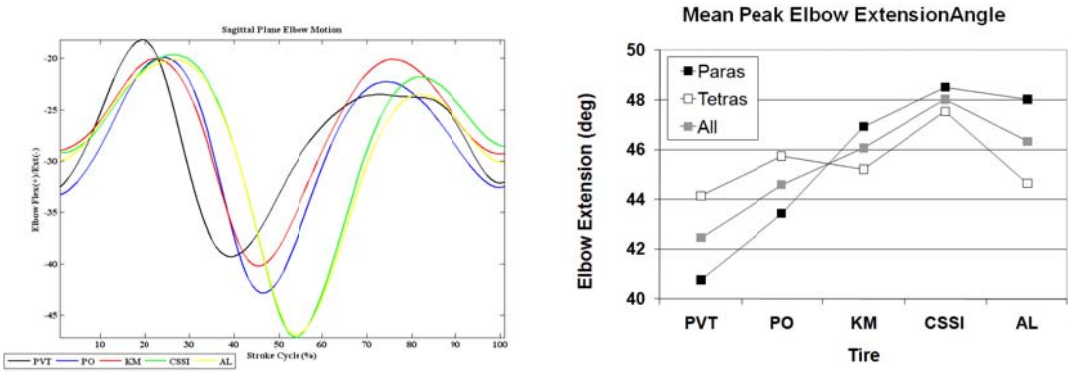

Figure 4.7 Sagittal plane elbow motion of participant P1 for each tire.

Table 4.4 Sagittal Plane Elbow Angles (degrees) for each Tire

Variable	Group	PVT	PO	KM	CSSI	AL
Minimum Extension	Para	-10.19 ± 7.38	-12.99 ± 7.69	-11.13 ± 7.89	-12.46 ± 7.23	-10.96 ± 7.58
	Tetra	-14.79 ± 6.96	-15.39 ± 6.86	-14.89 ± 8.96	-17.28 ± 7.82	-15.77 ± 7.40
	All	-12.49 ± 7.08	-14.19 ± 6.87	-13.01 ± 8.07	-14.87 ± 7.43	-13.36 ± 7.40
Maximum Extension	Para	-40.76 ± 10.37	-43.44 ± 4.96	-46.93 ± 10.58	-48.51 ± 7.38	-48.03 ± 9.95
	Tetra	-44.15 ± 7.58	-45.74 ± 6.33	-45.21 ± 8.00	-47.54 ± 7.19	-44.64 ± 10.38
	All	-42.46 ± 8.60	-44.59 ± 5.41	-46.07 ± 8.73	-48.03 ± 6.77	-46.33 ± 9.59
Range of motion	Para	30.58 ± 12.48	30.44 ± 9.97	35.80 ± 15.41	36.05 ± 12.02	37.06 ± 14.61
	Tetra	29.36 ± 8.81	30.35 ± 8.52	30.32 ± 10.53	30.26 ± 9.41	28.88 ± 9.45
	All	29.97 ± 10.02	30.40 ± 8.59	33.06 ± 12.57	33.15 ± 10.46	32.97 ± 12.20

Wrist Kinematics

For all participants sagittal plane wrist kinematics were characterized by peak extension shortly after initial contact, followed by wrist flexion during push phase. Wrist of flexion peaked at release and a returned to extension during recovery (Figure 4.5). While both groups increased wrist extension, paraplegic and tetraplegic participants showed opposite trends in peak wrist flexion in response to tires of increased rolling resistance. The paraplegic group exhibited an increase in peak flexion angle of 5.80 ± 11.21 degrees, while the tetraplegic group showed a 6.27 ± 5.71 decrease in peak flexion angle between the PVT and AL tires. This difference resulted in a large change in sagittal plane range of motion for individuals with paraplegia but little change for tetraplegic individuals. In the plane of ulnar and radial deviation, only ulnar deviation in the paraplegic group showed a consistent response to tires of increased rolling resistance.

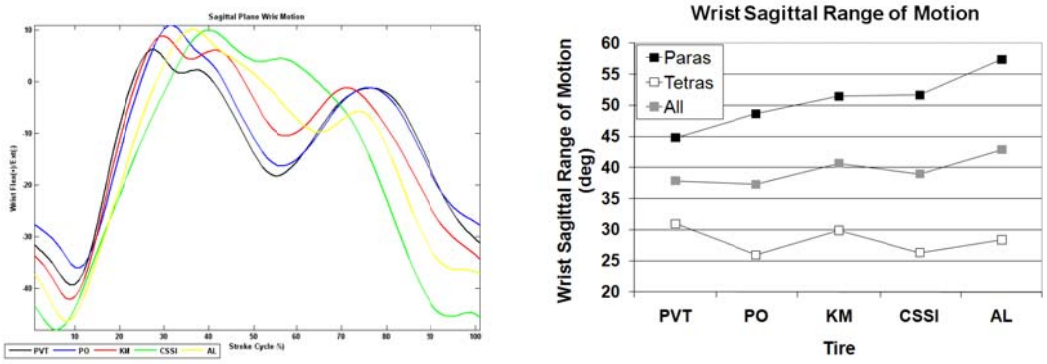

Figure 4.8 Sagittal plane wrist motion of participant T2 for each tire.

Table 4.5 Wrist Angles (degrees) for each Tire

Variable	Group	PVT	PO	KM	CSSI	AL
Maximum Flexion	Para	4.20.±12.71	4.62±12.75	5.05±11.71	6.56±14.09	10.00±10.39
	Tetra	-14.39±5.06	-14.82±7.98	-19.03±9.32	-18.37±3.78	-20.66±6.29
	All	-5.10±13.37	-5.10±14.32	-7.00±16.18	-5.90±16.39	-5.33±18.22
Maximum Extension	Para	40.63±8.98	44.04±7.52	46.41±6.56	45.11±6.13	47.40±6.55
	Tetra	45.35±15.85	40.77±10.11	48.92±11.27	44.67±13.87	49.07±17.19
	All	43.00±12.19	42.41±8.43	47.66±8.64	44.89±9.93	48.23±12.07
Flexion/Extension Range of Motion	Para	44.81±11.39	48.66±12.90	51.46±13.63	51.68±12.18	57.40±13.18
	Tetra	30.97±19.02	25.96±5.68	29.88±3.10	26.31±11.06	28.41±11.26
	All	37.89±16.29	37.31±15.24	40.67±14.72	38.99±17.32	42.91±19.21
Maximum Radial Deviation	Para	2.15±5.61	3.62±6.61	2.52±7.18	3.94±6.40	3.55±8.99
	Tetra	7.71±8.77	9.74±10.57	6.95±17.07	9.28±10.54	8.36±8.56
	All	4.93±7.44	6.68±8.79	7.96±12.21	6.61±8.56	5.95±8.53
Maximum Ulnar Deviation	Para	22.12±6.40	24.16±6.88	24.06±5.41	24.75±3.48	28.64±4.37
	Tetra	12.96±13.86	12.59±18.51	13.40±14.76	13.51±20.70	14.77±12.60
	All	17.54±11.13	18.37±14.33	15.50±14.86	19.13±15.00	21.71±11.46

CHAPTER 5

DISCUSSION

5.1 Participants

High variability of participant characteristics is a commonly cited difficulty in wheelchair propulsion research and makes comparisons across different studies challenging. In this study, participant characteristics other than tetraplegia or paraplegia were not controlled. Participants displayed great individual variation in body size, duration of injury and injury level. Tetraplegic participants were both heavier and more experienced wheelchair users than paraplegic participants. In Kwarciak et al. it was shown that the resistive force to propulsion increased with increased weight, particularly for solid tires [Kwarciak 2009]. The demand on the upper limb of participants with tetraplegia may have been greater for each tire simply due to greater mass, and therefore may have contributed to tetraplegic participants displaying generally slower self selected speed and greater push frequency. Greater mass could also have been responsible for negative effects on propulsion kinematics.

Previous studies have shown that more experienced wheelchair users generally display healthier propulsion technique and can more readily adapt their technique to different demands [Pentland 1994]. Though the tetraplegic group was injured for nearly twice as long as the paraplegic group, all participants have used a wheelchair for at least 3.5 years and would not be considered novice users. Therefore, it is not expected that years of wheelchair use would play a significant role in individual differences between participants or between the paraplegic and tetraplegic groups. Within the paraplegia

group, participants ranged in level of injury from T3 who would have little trunk control to T10 who would have at least partial trunk muscle innervation. Trunk control may have influenced biomechanics in this group but was not specifically examined in this study due to a small group size. Lastly, 3 of the 4 participants in the tetraplegia group were listed as C6/C7 neurological level of injury and may have had some residual but limited triceps control. For the purpose of this study the tetraplegia and paraplegia groups were interpreted as those with and those without any upper limb impairment respectively.

5.2 Temporal/Spatial Variables and Perceived Exertion

As participants propelled with tires of increased rolling resistance, they experienced a significant ($p < .05$) decrease in self-selected speed, comparable to the decrease that occurs when propelling over carpet or uphill [Newsam 1996, Koontz 2005, Richter 2007, Cowan 2008, Hurd 2008, Cowan 2009]. Participants with tetraplegia experienced a greater decrease in speed with more demanding propulsion due to higher rolling resistance tires than paraplegic participants. This finding is similar to previous findings that tetraplegic participants are unable to increase their speed to meet the demands of faster propulsion [Newsam 1996]. This decrease in speed could negatively affect community ambulation, particularly during extended wheeling, when fatigue could also be a factor. In order for manual wheelchair users to remain independent, they must be able to maintain a safe and functional speed [PVA 2005].

The use of higher rolling resistance tires also led to significantly increased push frequency ($p < .05$) and perceived exertion ($p \leq .035$). The effect of greater rolling resistance tires on push frequency was again greater for participants with tetraplegia than

participants with paraplegia. Given the association between high push frequency and repetitive strain injury of the upper limb [Dyson-Hudson 2004, van Drongelen 2005], manual wheelchair users are encouraged to reduce their rate of propulsion to help preserve upper limb function [PVA 2005, Cowan 2008]; however, this goal may be difficult to reach when propelling solid rear wheel tires with high rolling resistance. Minimal changes found in the spatial variables of propulsion is in agreement with the findings of Cowan et al., who concluded that during level propulsion push angle is independent of rolling resistance and is primarily a function of user-chair interface [Cowan 2009].

5.3 Stroke Pattern

Previous studies have found that individuals adapt their propulsion technique to changes in velocity and terrain [Newsam 1996, Richter 2007, Cowan 2009]. Three of the eight participants, all from the paraplegia group, modified their push pattern in response to greater rear wheel rolling resistance. It is important to consider the reasons and potential consequences of the changes. The three participants changed from either a single-looping over propulsion (SLOP) pattern or double-looping over propulsion (DLOP) pattern to an arcing pattern, when using a higher rolling resistance tire. These results are analogous to those presented in a study by Richter et al. in which persons with paraplegia who used a SLOP or DLOP pattern on level terrain changed to an arcing propulsion pattern when propelling up a 6° incline [Richter 2007]. The arcing pattern allows the hand to return to the wheel faster and remain in contact with the pushrim for a greater percentage of the stroke cycle; thus, it is used to compensate for increased loss of momentum when

propelling uphill [Richter 2007]. The arcing pattern has also been shown to be more metabolically efficient than any other pattern [de Groot 2004]. Despite the advantages in comfort and efficiency, the arcing pattern may lead to decreased propulsion effectiveness [Kwarciak 2009] and an increased risk of injury to the median nerve [Boninger 2002]. Manual wheelchair users are advised to use a pattern (semi-circular or DLOP) that leads to longer, smoother strokes [Newsam 1996, Boninger 2002], in order to preserve upper limb health.

Participants with tetraplegia were more resistant to change propulsion pattern when using tires with greater rolling resistance. Yet, like the paraplegia group, they decreased hand movement throughout propulsion. Greater resistance to adaptation with increased propulsion demands in individuals with tetraplegia is likely due upper impairments to limiting the range of possible positions. A more compact push stroke has been previous seen as an adaptation strategy used during propulsion up an incline [Chow 2009].

5.4 Kinematics

Trunk flexion has previously been found to increase with greater demand for force on the wheel. A flexed trunk position throughout propulsion is characteristic of uphill propulsion, propulsion across demanding terrain, and high speed propulsion [Veeger 1989, Richter 2007, Richter 2009]. In the present study, a more flexed trunk position was seen as tire rolling resistance increased. Rodgers et al. found that a more flexed trunk position was indicative of increased push frequency, increased VO_2 consumption, increased peak force on the pushrim, and fatigue. Although gas exchange and pushrim

force were not recorded in the current study, push frequency did increase, and it is reasonable to suspect that the use of tires with increased rolling resistance led to increased force on the pushrim [Rodgers 1994, Rodgers 2002].

Shoulder kinematics measured in this study have several marked differences to those found in previous research. Most notably many previous studies have found that at initial contact subjects displayed near maximum internal rotation and abduction and characterized the push phase as dominated by humeral movements in the direction of humeral external rotation, abduction and flexion [Rao 1996, Boninger 1998, Cooper 1999, Newsam 1999, Koontz 2002, Collinger 2008]. These studies also site peak internal rotation values near 90° and peak abduction above 70°. The humeral motion pattern and range of positions during push phase observed in this study was best characterized by humeral flexion accompanied by internal rotation and abduction. This motion pattern closely resembled the results found in Feng et al. [Feng 2010]. Shoulder angles in this study and in the Feng et al. study did not reach the extremes of the shoulder range of motion as was found by others [Feng 2010]. It is difficult to compare the results of shoulder kinematics between studies; differences between studies may result from differences in experimental setup, test conditions, individual participant characteristics, and definitions of coordinate systems among studies.

Shoulder motion was characterized by increased internal rotation as tire rolling resistance increased. Increases in internal rotation, combined with an expected increase in shoulder joint force, places the shoulder at greater risk of impingement [Mulroy 1996, Dyson-Hudson 2004, Mercer 2006, Collinger 2008]. The use of rear wheel tires with high rolling resistance, such as the Alshin tire, can expose the shoulder to greater stress at a

position of impingement. In the sagittal plane, increases in rolling resistance led to increased shoulder flexion and range of motion. Without additional information such as joint forces and muscle activity, it is difficult to interpret the implications of the increases; however, they seem to exemplify heightened efforts to overcome the additional resistance of solid tires.

In the group with paraplegia, increases in tire rolling resistance led to greater elbow extension near the point of release. This may indicate that the triceps were used to obtain the additional force needed to propel the tires with greater rolling resistance. Reduced innervation of the triceps in the tetraplegia group potentially prevented the use of this compensation strategy. The inability to increase the work of the triceps may be a factor in the greater relative speed loss with increased rolling resistance by the tetraplegia group relative to the group with paraplegia.

A substantial difference in the response of paraplegic versus participants with tetraplegia participants to increased rear wheel rolling resistance was also observed in wrist biomechanics. While both groups increased wrist extension, paraplegic participants exhibited an increase in peak flexion angle while the tetraplegic group showed decrease in peak flexion angle with tires of greater rolling resistance. This difference resulted in a large change in sagittal plane range of motion for individuals with paraplegia but little change for individuals with tetraplegia. In the plane of ulnar and radial deviation only ulnar deviation in the paraplegic group showed a consistent response to tires of increased rolling resistance. The most likely explanation for this is simply the participants with tetraplegia are unable to flex or deviate the wrist effectively due to impaired innervation of the necessary muscle groups. Greater wrist extension was seen by both groups in this

study with tires of greater rolling resistance. Wrist extension has been previously associated with greater pressure in the carpal tunnel and is thought to influence median nerve injury [Boninger 2004]. Boninger et al. reported a smaller range of motion at the wrist was associated with a larger incidence of pain but concluded this was due to the relationship of smaller wrist range and increased cadence and forces [Boninger 2004]. A smaller range of motion accompanied by greater overall wrist extension as was seen in the tetraplegic group, putting the user in a high risk position for nerve injury. This suggests a second possible explanation for the association seen in the Boninger et al. study.

5.5 Limitations

There were several limitations to this study. First, the rolling resistances presented in this study (obtained from previous coast-down tests) were associated with each tire, independent of the participants. Determining the precise resistance experienced by each participant would allow for direct correlations of rolling resistance with the outcome variables. The range of rolling resistances could also be expanded by testing additional tires. Second, only eight participants were tested. Future studies of tires should include a greater population of users. Third, standard wheels were used as opposed to instrumented wheels; therefore, the forces and moments on the upper limbs could not be determined. Lastly participants self reported level of injury. A formal assessment of motor function shoulder be completed to determine level of injury in future research.

An additional limitation was observed in the results. When propelling the KIK Mako tire, participants exhibited biomechanics more closely associated with the Primo

V-Trak tire (lower rolling resistance) than with the other solid tires or the Primo Orion tire (most similar rolling resistance). The KIK Mako was the only low-profile tire besides the Primo V-Trak tested in this study. Based on rolling resistance, the unexpected biomechanics associated with the KIK Mako could be an effect of the profile type or diameter. The design of the study was not to evaluate tire design, thus, further research is needed to confirm this relationship.

CHAPTER 6

CONCLUSIONS

The results of this study clearly demonstrate distinct trends in wheelchair propulsion biomechanics resulting from the use of rear wheel tires of different rolling resistances. Creating a more compact push stroke by increasing forward lean, shortening the hand path and reducing recovery time proved to be the primary strategy employed by the participants to overcome the demands of wheelchair propulsion with tires of greater rolling resistance. This change in propulsion strategy is analogous to the change employed by wheelchair users to propel up a slope as observed by Chow et al. [Chow 2009]. Propulsion with higher rolling resistance tires resulted in biomechanics often associated with repetitive strain injury of the upper limb including increased push frequency and decreased self selected speed as well as limb positions associated with impingement.

By thoroughly evaluating the effect of rear tire choice on the risk for upper limb injury, an educated decision can be made on the most appropriate tire for a given individual. Although additional factors, such as the need for traction on uneven terrain or the need for low maintenance, will factor into the choice of rear wheel tire, a clinician or wheelchair user should place these needs in perspective with the effect of tire choice on upper limb health. This is especially true for individuals found to be at greater risk for pain such as those individuals who are older, have been injured longer, have higher neurological levels of injury or have an unhealthy BMI. For these individuals a low

profile high pressure pneumatic tire is highly recommended to reduce the demands on the upper limb.

Wheelchair propulsion research, regardless of its focus, should consider the impact of tire selection. In particular, research conducted with instrumented wheels equipped with the Alshin tire must account for the impact of the high rolling resistance tire on all measurements. Unfortunately, in much of the literature to date tire type is often omitted. The results of this study show that it is important for the research community to list tire type as part of the study set-up and equipment. Future studies on the effects of rear tire type should focus on differences in demands on the upper limb when using different tires. In order to create a comprehensive understanding of these demands, kinematics, kinetics, and electromyography of the upper limb, as well as physical capacity of the wheelchair user, should be measured. A greater understanding of the impact of tire type may also help drive the industry to create new products that meet the performance needs of users (traction and durability) while minimizing the harmful impacts on upper limb health.

APPENDIX A

PARTICIPANT KINEMATIC DATA

Appendix A includes all participant kinematic data.

			Trunk		Shoulder						Elbow		Wrist			
			Flex(+)/Ext(-)		Add(+)/Abd(-)		Inrot(+)/Exrot(-)		Flex(+)/Ext(-)		Flex(+)/Ext(-)		Flex(+)/Ext(-)		Rad(+)/Uln(-)	
			Min	Max	Min	Max	Min	Max	Min	Max	Min	Max	Min	Max	Min	Max
AC	HPPT	Mean	**-0.59**	**10.19**	**-27.50**	**-20.26**	**-6.07**	**15.62**	**-50.20**	**3.87**	**-39.90**	**-0.54**	**-34.46**	**21.18**	**-28.49**	**3.78**
		STD	1.27	1.82	1.76	0.64	4.42	4.24	1.22	4.47	7.60	0.50	2.52	1.10	1.70	2.08
	LPPT	Mean	**-0.94**	**10.66**	**-33.92**	**-20.68**	**8.50**	**21.68**	**-47.23**	**4.52**	**-43.07**	**-1.96**	**-47.12**	**19.20**	**-33.12**	**2.47**
		STD	1.24	0.90	2.48	3.06	1.35	3.55	1.67	3.42	10.31	1.67	3.60	2.39	1.12	0.61
	KT	Mean	**-4.25**	**8.62**	**-25.92**	**-16.90**	**-1.68**	**14.52**	**-50.85**	**7.13**	**-49.88**	**-0.87**	**-48.39**	**19.73**	**-29.23**	**1.98**
		STD	0.74	0.79	1.61	1.68	2.71	1.68	1.32	5.23	7.26	1.61	3.28	1.97	1.10	0.99
	SI	Mean	**-3.08**	**10.05**	**-30.08**	**-17.50**	**-1.81**	**17.62**	**-48.99**	**10.48**	**-55.15**	**-2.68**	**-39.02**	**24.98**	**-28.98**	**4.64**
		STD	1.36	1.36	2.71	1.74	5.90	1.93	1.57	3.93	4.30	1.18	4.10	4.51	2.24	1.92
	SW	Mean	**-0.55**	**12.04**	**-34.21**	**-17.96**	**3.90**	**19.54**	**-49.09**	**9.97**	**-54.58**	**-1.82**	**-48.91**	**24.64**	**-34.44**	**2.20**
		STD	0.92	1.39	2.00	0.98	3.80	1.01	0.25	2.58	2.77	0.82	4.66	2.67	2.10	1.33
IB	HPPT	Mean	**-15.23**	**-14.15**	**-34.73**	**-27.35**	**18.11**	**26.55**	**-54.28**	**-28.21**	**-35.04**	**-8.75**	**-53.56**	**-5.28**	**-22.96**	**-5.49**
		STD	1.05	1.11	2.98	1.33	3.38	4.74	1.75	5.71	2.56	1.39	3.59	2.66	2.36	0.48
	LPPT	Mean	**-14.69**	**-11.60**	**-36.82**	**-24.47**	**24.09**	**42.30**	**-50.60**	**-4.46**	**-45.10**	**-14.51**	**-53.02**	**-7.54**	**-24.30**	**-4.33**
		STD	1.57	1.17	1.86	1.55	0.61	5.15	1.35	3.12	1.66	1.16	1.29	4.07	1.27	0.47
	KT	Mean	**-16.52**	**-13.84**	**-37.05**	**-27.28**	**20.32**	**35.12**	**-51.99**	**-10.64**	**-40.46**	**-10.87**	**-54.78**	**-3.11**	**-25.15**	**-6.03**
		STD	0.71	1.55	1.92	1.00	1.48	6.49	2.27	2.38	1.90	1.52	1.52	2.98	1.49	0.67
	SI	Mean	**-14.78**	**-13.03**	**-37.39**	**-26.19**	**21.19**	**31.73**	**-50.66**	**-21.34**	**-38.71**	**-11.97**	**-52.11**	**-4.37**	**-24.02**	**-2.77**
		STD	0.69	0.47	1.65	0.85	3.02	3.79	1.27	2.59	3.51	0.87	1.58	1.70	1.90	1.36
	SW	Mean	**-14.44**	**-10.01**	**-37.91**	**-24.73**	**21.23**	**35.83**	**-52.76**	**-11.66**	**-37.49**	**-9.42**	**-55.04**	**3.13**	**-27.98**	**-5.80**
		STD	0.67	1.53	2.30	1.04	3.27	4.53	3.00	3.85	4.66	3.28	2.52	1.91	1.53	0.80
LM	HPPT	Mean	**-4.93**	**0.64**	**-19.74**	**-7.63**	**5.51**	**39.63**	**-44.76**	**6.68**	**-55.62**	**-13.84**	**-39.91**	**6.63**	**-23.78**	**2.37**
		STD	0.81	0.44	1.29	1.19	2.65	2.83	0.60	2.80	5.18	0.57	1.89	1.73	1.21	1.71
	LPPT	Mean	**-2.22**	**2.57**	**-19.54**	**-6.17**	**1.20**	**34.97**	**-44.22**	**0.61**	**-48.71**	**-15.75**	**-36.15**	**11.31**	**-22.80**	**4.62**
		STD	1.75	1.85	1.09	2.01	2.20	3.29	1.32	3.19	5.04	0.92	1.48	1.32	0.87	1.34
	KT	Mean	**-3.30**	**2.87**	**-18.46**	**-5.98**	**3.47**	**38.16**	**-43.33**	**9.58**	**-60.51**	**-12.80**	**-42.18**	**9.15**	**-25.39**	**2.61**
		STD	0.56	0.51	1.36	0.41	1.15	2.05	0.32	2.14	3.29	0.74	2.57	1.65	0.99	0.66
	SI	Mean	**-4.57**	**0.40**	**-23.26**	**-10.09**	**11.96**	**43.44**	**-39.79**	**2.15**	**-53.13**	**-15.56**	**-48.29**	**10.20**	**-25.44**	**1.49**
		STD	1.15	1.59	1.61	1.13	5.80	3.20	0.97	3.67	5.34	0.96	5.75	4.04	1.14	2.85
	SW	Mean	**0.96**	**6.14**	**-23.18**	**-6.24**	**6.76**	**44.43**	**-41.50**	**8.21**	**-58.24**	**-12.48**	**-46.43**	**10.13**	**-28.31**	**1.96**
		STD	1.04	1.55	1.62	1.04	1.88	3.94	1.16	2.20	3.24	1.41	1.34	2.14	1.40	1.19
WE	HPPT	Mean	**-2.57**	**3.99**	**-22.35**	**-20.24**	**16.18**	**24.93**	**-39.11**	**-15.48**	**-32.50**	**-17.61**	**-34.61**	**-5.82**	**-13.24**	**7.93**
		STD	2.77	1.60	1.15	0.71	1.03	3.15	1.01	6.11	1.46	0.98	1.57	6.37	4.77	1.56
	LPPT	Mean	**-0.22**	**9.51**	**-25.35**	**-21.12**	**18.19**	**32.75**	**-35.39**	**-0.20**	**-36.86**	**-19.76**	**-39.88**	**-4.47**	**-16.41**	**11.72**
		STD	1.06	0.83	0.73	0.89	2.19	0.91	0.80	2.15	1.31	1.82	1.00	1.08	1.02	1.02
	KT	Mean	**-4.36**	**4.94**	**-21.44**	**-16.90**	**15.65**	**28.65**	**-36.87**	**-2.15**	**-36.87**	**-19.98**	**-40.30**	**-5.56**	**-16.44**	**11.53**
		STD	1.03	0.73	0.90	0.69	1.48	0.83	0.62	0.98	1.07	1.01	1.24	0.80	0.63	1.54
	SI	Mean	**-2.40**	**7.44**	**-23.08**	**-16.05**	**17.18**	**36.07**	**-35.43**	**3.13**	**-47.05**	**-19.64**	**-41.03**	**-4.56**	**-20.57**	**12.39**
		STD	1.03	0.65	1.14	0.62	1.89	1.41	0.58	0.73	1.22	0.55	1.84	1.72	0.96	1.56
	SW	Mean	**-5.27**	**1.84**	**-22.38**	**-17.91**	**19.86**	**35.28**	**-37.15**	**-1.52**	**-41.79**	**-20.13**	**-39.22**	**2.11**	**-23.84**	**5.83**
		STD	0.77	0.54	0.89	0.64	0.96	2.17	0.93	1.87	1.30	1.04	0.93	1.45	0.72	1.19
BD	HPPT	Mean	**4.52**	**8.87**	**-42.91**	**-32.74**	**32.68**	**54.14**	**-37.38**	**0.12**	**-34.81**	**-18.16**	**-68.64**	**-9.60**	**6.13**	**16.05**
		STD	0.43	0.51	1.58	1.37	0.42	0.82	1.51	1.07	0.78	1.76	1.95	3.68	0.88	2.72
	LPPT	Mean	**1.18**	**9.95**	**-42.37**	**-31.06**	**20.38**	**57.17**	**-41.22**	**1.97**	**-37.57**	**-17.25**	**-54.96**	**-24.97**	**13.86**	**22.44**
		STD	1.15	1.59	0.59	2.25	6.11	1.44	3.24	1.07	2.31	1.13	2.13	3.11	2.25	1.12
	KT	Mean	**5.22**	**8.98**	**-42.32**	**-33.09**	**36.49**	**56.07**	**-34.20**	**2.12**	**-35.49**	**-20.00**	**-64.57**	**-31.64**	**18.35**	**28.82**
		STD	0.65	0.97	1.32	0.83	0.84	2.03	1.34	1.36	0.73	0.79	1.17	3.39	1.00	1.22
	SI	Mean	**9.10**	**21.44**	**-46.48**	**-33.22**	**35.23**	**61.61**	**-29.05**	**7.73**	**-37.18**	**-16.34**	**-64.09**	**-21.48**	**14.19**	**22.46**
		STD	0.25	0.54	0.78	0.67	2.49	2.19	1.66	0.98	0.89	1.39	2.22	7.20	1.56	1.01
	SW	Mean	**13.00**	**19.13**	**-47.67**	**-34.39**	**33.75**	**68.28**	**-29.77**	**12.02**	**-31.41**	**-15.20**	**-73.31**	**-28.35**	**1.14**	**8.42**
		STD	1.07	1.41	1.06	0.83	1.09	2.80	1.43	2.03	3.62	1.53	2.19	11.83	7.81	1.24
BM	HPPT	Mean	**-12.12**	**-1.78**	**-22.43**	**-16.88**	**19.65**	**30.51**	**-46.01**	**-14.14**	**-52.82**	**-22.61**	**-33.09**	**-13.38**	**-18.13**	**7.36**
		STD	1.04	1.00	2.06	1.06	3.95	4.76	0.67	1.31	1.36	2.11	3.01	0.63	0.73	2.06
	LPPT	Mean	**-10.49**	**0.09**	**-26.25**	**-18.06**	**25.92**	**32.34**	**-44.13**	**-13.74**	**-52.22**	**-23.97**	**-31.02**	**-10.09**	**-21.25**	**7.42**
		STD	0.68	1.56	2.13	0.75	2.91	2.34	1.17	1.40	2.38	1.05	2.51	1.80	1.57	2.97
	KT	Mean	**-12.23**	**-5.82**	**-22.42**	**-15.55**	**23.51**	**28.54**	**-47.29**	**-14.02**	**-54.92**	**-24.74**	**-38.29**	**-11.86**	**-18.81**	**9.25**
		STD	1.03	0.59	0.96	1.25	1.07	4.21	1.16	1.63	1.05	1.29	1.55	1.19	1.63	2.30
	SI	Mean	**-7.11**	**1.60**	**-28.49**	**-18.07**	**25.25**	**39.18**	**-42.74**	**-9.79**	**-52.86**	**-28.40**	**-31.54**	**-12.87**	**-24.84**	**7.93**
		STD	1.36	1.91	1.35	1.30	3.57	3.02	2.20	1.22	2.96	1.75	1.80	4.16	1.10	1.69
	SW	Mean	**-6.59**	**4.49**	**-25.80**	**-16.31**	**26.45**	**48.23**	**-42.91**	**-10.14**	**-55.99**	**-26.30**	**-33.90**	**-13.66**	**-28.45**	**8.20**
		STD	1.23	1.98	2.30	1.27	3.73	8.84	2.65	0.66	2.22	1.49	2.65	2.33	2.04	0.60
JM	HPPT	Mean	**-5.53**	**4.70**	**-18.52**	**-10.58**	**3.73**	**17.85**	**-47.16**	**-15.40**	**-46.73**	**-11.44**	**-40.29**	**-21.53**	**-26.55**	**11.76**
		STD	0.46	0.63	0.47	0.63	1.73	7.29	1.15	2.25	0.79	1.17	1.55	2.44	2.03	1.25
	LPPT	Mean	**-7.64**	**3.72**	**-19.13**	**-10.40**	**1.55**	**17.28**	**-47.31**	**-13.71**	**-44.36**	**-12.37**	**-38.36**	**-17.14**	**-28.36**	**12.11**
		STD	0.65	0.88	1.20	0.78	1.73	8.81	0.43	2.14	0.59	0.51	0.99	2.72	1.80	0.56
	KT	Mean	**-4.64**	**3.87**	**-20.34**	**-11.87**	**0.32**	**12.20**	**-48.34**	**-17.05**	**-46.50**	**-9.13**	**-48.64**	**-20.51**	**-14.86**	**20.69**
		STD	1.02	0.72	1.22	1.14	0.83	1.59	0.37	1.35	2.41	0.45	1.58	0.63	1.64	0.73
	SI	Mean	**-7.33**	**10.32**	**-23.23**	**-9.45**	**0.44**	**24.79**	**-46.49**	**-8.00**	**-48.21**	**-14.07**	**-39.58**	**-19.23**	**-33.02**	**9.99**
		STD	0.34	0.69	0.82	0.41	0.63	0.81	0.88	0.54	1.27	0.72	2.36	3.20	1.58	0.68
	SW	Mean	**-5.13**	**8.66**	**-24.03**	**-11.29**	**3.90**	**21.36**	**-47.44**	**-10.54**	**-42.61**	**-12.08**	**-48.27**	**-22.57**	**-19.98**	**18.89**
		STD	0.58	0.46	0.67	0.35	1.45	1.09	0.34	0.73	0.80	0.84	1.68	2.60	0.87	0.93
TDH	HPPT	Mean	**-4.04**	**7.69**	**-17.71**	**-4.16**	**2.84**	**30.89**	**-37.86**	**5.14**	**-42.26**	**-6.94**	**-39.39**	**-13.03**	**-13.29**	**-4.31**
		STD	0.65	0.22	0.48	0.88	2.31	1.24	0.56	1.42	2.22	1.01	0.84	2.10	0.86	0.80
	LPPT	Mean	**-2.15**	**9.43**	**-16.98**	**-1.31**	**-0.17**	**29.66**	**-36.36**	**8.38**	**-48.83**	**-7.99**	**-38.75**	**-7.07**	**-14.60**	**-3.03**
		STD	0.78	0.33	0.55	0.87	0.69	2.03	0.64	0.80	2.37	0.51	2.40	2.37	1.12	1.57
	KT	Mean	**-4.77**	**7.12**	**-18.30**	**-3.74**	**1.85**	**30.41**	**-39.09**	**4.25**	**-43.95**	**-5.69**	**-44.15**	**-12.12**	**-12.48**	**-5.18**
		STD	0.47	0.48	0.61	0.75	1.19	1.48	0.40	0.55	2.33	1.66	0.94	0.92	0.49	1.16
	SI	Mean	**-2.60**	**10.49**	**-18.51**	**-4.33**	**5.37**	**35.82**	**-37.50**	**7.82**	**-51.90**	**-10.32**	**-43.48**	**-19.89**	**-10.37**	**-3.26**
		STD	1.10	0.77	0.71	0.67	1.02	1.51	1.86	1.80	2.91	2.32	0.40	5.41	0.64	0.82
	SW	Mean	**-3.55**	**7.84**	**-17.32**	**-4.98**	**4.81**	**33.76**	**-38.79**	**5.85**	**-48.56**	**-9.48**	**-40.79**	**-18.06**	**-11.77**	**-2.07**
		STD	0.74	1.70	0.75	0.79	0.72	0.73	1.08	1.27	1.23	1.33	0.78	5.49	1.74	1.26

APPENDIX B

JOINT ANGLE CALCULATIONS THEORY

For each segment the rotation matrix is made from the coordinate axes of the segement shown in code lines ~126-148 of the joint angle calculation programs. The transformation matrix is then found by multiplying the inverse of the proximal segment rotation matrix by the distal segment rotation matrix. The transformation matrix is resolved by combining the three rotation matrices associated with each individual rotation in the ZXY order as follows:

X rotation matrix

$$[rx,\alpha] = \begin{vmatrix} 1 & 0 & 0 \\ 0 & \cos(\alpha) & \sin(\alpha) \\ 0 & -\sin(\alpha) & \cos(\alpha) \end{vmatrix}$$

Y rotation matrix

$$[ry,\beta] = \begin{vmatrix} \cos(\beta) & 0 & -\sin(\beta) \\ 0 & 1 & 0 \\ \sin(\beta) & 0 & \cos(\beta) \end{vmatrix}$$

Z rotation matrix

$$[rz,\gamma] = \begin{vmatrix} \cos(z) & \sin(z) & 0 \\ -\sin(z) & \cos(z) & 0 \\ 0 & 0 & 1 \end{vmatrix}$$

Therefore, the transformation matrix $[Tzxy] = [rz,\gamma]*[rx,\alpha]*[ry,\beta]$

$$[Tzxy] = \begin{vmatrix} (c(\gamma)*c(\beta)-s(\gamma)*s(\alpha)*s(\beta)) & -s(\gamma)*c(\beta) & (c(\gamma)*s(\beta)+s(\gamma)*s(\alpha)*c(\beta)) \\ (s(\gamma)*c(\beta)-c(\gamma)*s(\alpha)*s(\beta)) & c(\gamma)*c(\beta) & (s(\gamma)*s(\beta)-c(\gamma)*s(\alpha)*c(\beta)) \\ -c(\alpha)*s(\beta)) & s(\alpha) & c(\alpha))*c(\beta)) \end{vmatrix}$$

Using the transformation matrix [Tzxy] the alpha angle can be solved for by taking the arccosine of the value in position 3,2 of the transformation matrix as is done in line 172 of the code for each of the joint angle calculation programs. ZXY rotation was chosen to give priority to the sagittal plane rotation (flexion/extension) which is the angle of greatest interest.

Programming

Programs used in kinematic analysis: TetraKinematics5SC.m, trunktoglobalISB.m, humtotrunkISB.m, foretohum.m, wristtofore.m, fivepsmeanSC.m, resample1to101.m, angularVandA.m

The following programs are explained in a top down fashion.

Master Program

TetraKinemtics5SC.m – The main function and interface for analysis of tetraplegia kinematic data. This program allows user to select subject and file to be analyzed and loads previously preprocessed data. Functions to calculate joint angles are called from this program (*trunktoglobalISB.m, humtotrunkISB.m, foretohum.m, wristtofore.m*). Data is normalized to 100% of the stroke cycle using the *resample1to101*.m and *fivepsmeanSC.m* programs. Joint angular velocity and angular accelerations are calculated using the *angularVandA.m* program. All plotting and variable saving is conducted.

Joint Angle Calculations

trunktoglobalISB.m – This program calculates the following tri-planar angles of the trunk coordinate system (ISB standard) referenced to the laboratory global coordinate system.

1. Sagittal Plane: Rotation about Z (gamma angle) – trunk flexion(+)/extension(-)
2. Frontal Plane: Rotation about X (alpha angle) – trunk lateral bending right(+)/left(-)
3. Transverse Plane: Rotation about Y (beta angle) – trunk torsion L(+)/R(-)

humtotrunkISB.m – This program calculates the following tri-planar angles of the humerus coordinate system (ISB standard) rotated to the trunk coordinate system (ISB standard).

1. Sagittal Plane: Rotation about Z (gamma angle) – shoulder flexion(+)/extension(-)
2. Frontal Plane: Rotation about X (alpha angle) – shoulder abduction(+)/adduction(-)

3. Transverse Plane: Rotation about Y (beta angle) – shoulder internal rotation(+)/external rotation(-)

foretohum.m – This program calculates the following tri-planar angles of the forearm coordinate system (ISB standard) rotated to the humerus coordinate system (ISB standard).

1. Sagittal Plane: Rotation about Z (gamma angle) – elbow flexion(+)/extension(-)
2. Frontal Plane: Rotation about X (alpha angle) – ignored
3. Transverse Plane: Rotation about Y (beta angle) – pronation(+)/ supination(-)

wristtofore.m – This program calculates the following tri-planar angles of the hand coordinate system (ISB standard) rotated to the forearm coordinate system (ISB standard).

1. Sagittal Plane: Rotation about Z (gamma angle) – wrist flexion(+)/extension(-)
2. Frontal Plane: Rotation about X (alpha angle) – Wrist Radial Deviation(+)/Ulnar Deviation(-)
3. Transverse Plane: Rotation about Y (beta angle) – ignored (should be close to zero as the hand should rotate with the same angle as the forearm)

Other Programs

fivepsmeanSC.m – This program divides the data into 5 stroke cycles based on the on/off points determined during preprocessing and controls data plotting. The program calls *resample1to101.m.*

resample1to101.m – Normalizes selected data to 101 points using the built in Matlab function resample.m

REFERENCES

Aissaoui R, Desroches G. Stroke pattern classification during manual wheelchair propulsion in the elderly using fuzzy clustering. J Biomech. 2008 Aug;41:2438–2445

Aljure J, Eltorai I, Bradley WE, Lin JE, Johnson B. Carpal tunnel syndrome in paraplegic patients. Paraplegia 1985;23:182-186.

An KN, Browne AO, Korinek S, Tanaka S, Morrey BF. Three-dimensional kinematics of glenohumeral elevation. J Orthop Res. 1991 Jan;9(1):143-149.

Bayley JC, Cochran TP, Sledge CB The weight-bearing shoulder: the impingement syndrome in paraplegics. Journal of Bone & Joint Surgery. 1987;69:676–678.

Bednarczyk JH, Sanderson DJ. Kinematics of wheelchair propulsion in adults and children with spinal cord injury. Arch Phys Med Rehabil. 1994 Dec;75(12):1327-1334.

Beekman CE, Miller-Porter L, Schoneberger M. Energy cost of propulsion in standard and ultralight wheelchairs in people with spinal cord injuries. Phys Ther 1999;79:146–158.

Boninger ML, Baldwin M, Cooper RA, Koontz A, Chan L. Manual wheelchair pushrim biomechanics and axle position. Arch Phys Med Rehabil 2000;81:608-613.

Boninger ML, Cooper RA, Shimada SD, Rudy TE Shoulder and elbow motion during two speeds of wheelchair propulsion: a description using a local coordinate system. Spinal Cord. 1998 Jun;36(6):418-426.

Boninger ML, Impink BG, Cooper RA, Koontz AM. Relation between median and ulnar nerve function and wrist kinematics during wheelchair propulsion. Arch Phys Med Rehabil. 2004 Jul;85(7):1141-1145.

Boninger ML, Souza AL, Cooper RA, Fitzgerald SG, Koontz AM, Fay BT. Propulsion patterns and pushrim biomechanics in manual wheelchair propulsion. Arch Phys Med Rehabil. 2002;83:718–723

Boninger ML, Towers JD, Cooper RA, Dicianno BE, Munin MC. Shoulder imaging abnormalities in individuals with paraplegia. Journal of Rehabilitation R&D. 2001;38:401–408.

Borg G. Borg's Perceived Exertion and Pain Scales. Champlain, IL: Human Kinetics; 1988:29-38.

Browne AO, Hoffmeyer P, Tanaka S, An KN, Morrey BF. Glenohumeral elevation studied in three dimensions. J Bone Joint Surg Br. 1990 Sep;72(5):843-5.

Brubaker CE. Wheelchair prescription: an analysis of factors that affect mobility and performance. J Rehabil Res Dev 1986;23(4):19-26.

Burnham RS, Steadward RD. Upper extremity peripheral nerve entrapments among wheelchair athletes: prevalence, location, and risk factors. Arch Phys Med Rehabil 1994;75:519-524.

Chow JW, Millikan TA, Carlton LG, Chae WS, Lim YT, Morse MI.Kinematic and electromyographic analysis of wheelchair propulsion on ramps of different slopes for young men with paraplegia.Arch Phys Med Rehabil 2009 Feb;90(2):271-278.

Collinger JL, Boninger ML, Koontz AM, Price R, Sisto SA, Tolerico ML, Cooper RA. Shoulder biomechanics during the push phase of wheelchair propulsion: a multi-site study of persons with paraplegia. Arch Phys Med Rehabil. 2008; 89:667-676.

Cooper RA, Boninger ML, Shimada SD, Lawrence BM. Glenohumeral joint kinematics and kinetics for three coordinate system representations during wheelchair propulsion. Am J Phys Med Rehabil. 1999 Sep-Oct;78(5):435-446.

Cowan R, Nash M, Collinger J, Koontz A, Boninger ML. Impact of Surface Type, Wheelchair Weight, and Axle Position on Wheelchair Propulsion by Novice Older Adults Archives of Physical Medicine and Rehabilitation 2009 July;90(2) 1076-1083.

Cowan RE, Boninger ML, Sawatzky BJ, Mazoyer BD, Cooper RA.Preliminary outcomes of the SmartWheel Users' Group database: a proposed framework for clinicians to objectively evaluate manual wheelchair propulsion. Arch Phys Med Rehabil 2008 Feb;89(2):260-268.

Curtis K, Drysdale G, Lanza D, Kolber M, Vitolo R, West R. Shoulder Pain in Wheelchair Users with Tetraplegia and Paraplegia. Arch Phys Med Rehabil. 1999;80:453-457.

Curtis K.A, Tyner T.M, Zachary L, Lentell G, Brink D, Didyk T, Gean K, Hall J, Hooper M, Klos J, Lesina S, Pacillas B. Effect of a standard exercise protocol on shoulder pain in long-term wheelchair users. Spinal Cord. 1999;37:421–429.

Curtis KA, Development of the Wheelchair User's Shoulder Pain Index (WUSPI). Paraplegia, 1995a. 33(5):90-293.

Dalyan M, Cardenas DD, Gerard B. Upper extremity pain after spinal cord injury. Spinal Cord. 1999;37:191-195.

Davidoff G, Werner R, Waring W. Compressive mononeuropathies of the upper extremity in chronic paraplegia. Paraplegia 1991;29:17-24.

Davis JL, Growney ES, Johnson ME, Iuliano BA, An KN. Three-dimensional kinematics of the shoulder complex during wheelchair propulsion: a technical report.J Rehabil Res Dev. 1998 Jan;35(1):61-72.

de Groot S, Dallmeijer AJ, Kilkens OJ, van Asbeck FW, Nene AV, Angenot EL, Post MW, van der Woude LH. Course of gross mechanical efficiency in handrim wheelchair propulsion during rehabilitation of people with spinal cord injury: a prospective cohort study. Arch Phys Med Rehabil. 2005 Jul;86(7):1452-1460.

de Groot S, Veeger HE, Hollander AP, Van der Woude LH. Effect of wheelchair stroke pattern on mechanical efficiency. Am J Phys Med Rehabil. 2004;83:640–649

Delgrosso I, Boillat MA. Carpal tunnel syndrome: role of occupation. Int Arch Occup Environ Health 1991 ;63:267-270.

Dyson-Hudson A, Kirshblum SC. Shoulder pain in chronic spinal cord injury, part 1: epidemiology, etiology, and pathomechanics. J Spinal Cord Med. 2004;27:4-17.

Escobedo EM, Hunter JC, Hollister MC, Patten RM, Goldstein B. AJR Am J Roentgenol. 1997 MR imaging of rotator cuff tears in individuals with paraplegia. Apr;168(4):919-923.

Feng CK, Wei SH, Chen WY, Lee HC, Yu CH. Comparing the shoulder impingement kinematics between circular and pumping strokes in manual wheelchair propulsionDisability and Rehabilitation: Assistive Technology, November 2010; 5(6): 448–455

Finley MA, Rasch EK, Keyser RE, Rodgers MM. The biomechanics of wheelchair propulsion in individuals with and without upper-limb impairment. J Rehabil Res Dev. 2004 May;41(3B):385-395.

Finley MA, Rodgers MM, Rasch EK, McQuade KJ, Keyser RE. Reliability of biomechanical variables during wheelchair ergometry testing. J Rehabil Res Dev. 2002 Jan-Feb;39(1):73-81.

Gellman H, Chandler DR, Petrasek J, Sie I, Adkins R, Waters RL. Carpal tunnel syndrome in paraplegic patients. J Bone Joint Surg Am 1988;70:517-519.

Gellman H, Sie I, Waters RL. Late complications of the weight-bearing upper extremity in the paraplegic patient. Clin Orthop. 1988;223:132-135

Gordon J, Kauzlarich, JJ, Thacker, JG. Tests of two new polyurethane foam wheelchair tires. J Rehabil Res Dev. 1989;26(1):33-46.

Gutierrez DD, Mulroy SJ, Newsam CJ, Gronley JK, Perry J. Effect of fore-aft seat position on shoulder demands during wheelchair propulsion: part 2. An electromyographic analysis. J Spinal Cord Med 2005;28(3):222-229.

Herring SA, Nilson KL. Introduction to overuse injuries. Clin Sports Med. 1987;6:225-239

Hilbers PA, White TP. Effects of wheelchair design on metabolic and heart rate responses during propulsion by persons with paraplegia. Phys Ther 1987;67:1355–1358.

Hughes CJ, Weimar WH, Sheth PN, Brubaker CE. Biomechanics of wheelchair propulsion as a function of seat position and user-to-chair interface. Arch Phys Med Rehabil 1992;73(3):263-269.

Hurd WJ, Morrow MM, Kaufman KR, An KN. Influence of varying level terrain on wheelchair propulsion biomechanics. Am J Phys Med Rehabil. 2008 Dec;87(12):984-991.

Katz JN, Simmons BP. Clinical practice. Carpal tunnel syndrome. N Engl J Med. 2002 Jun 6;346(23):1807-1812.

Kauzlarich JJ, Thacker JG. Wheelchair tire rolling resistance and fatigue. J Rehabil Res Dev. 1985;22(3):25-41.

Kaye HS, Kang T, and LaPlante MP. Wheelchair users in the United States. Disability Statistics Center, Institute for Health and Aging, School of Nursing. 2002, University of California: San Francisco.

Kendall FP, McCreary EK, Provance PG. Muscles: Testing and Function With Posture and Pain. Lippincott Williams & Wilkins. 2005

Koontz AM, Cooper RA, Boninger ML, Souza AL, Fay BT. Shoulder kinematics and kinetics during two speeds of wheelchair propulsion. J Rehabil Res Dev. 2002 Nov-Dec;39(6):635-649.

Koontz AM, Cooper RA, Boninger ML, Yang Y, Impink BG, van der Woude LH. A kinetic analysis of manual wheelchair propulsion during start-up on select indoor and outdoor surfaces. J Rehabil Res Dev 2005;42:447-458.

Koontz AM, Roche BM, Collinger JL, Cooper RA, Boninger ML. Manual wheelchair propulsion patterns on natural surfaces during start-up propulsion. Arch Phys Med Rehabil. 2009 Nov;90(11):1916-1923.

Kotajarvi BR, Sabick MB, An KN, Zhao KD, Kaufman KR, Basford JR. The effect of seat position on wheelchair propulsion biomechanics. J Rehabil Res Dev 2004;41(3B): 403-414.

Kulig K, Newsam CJ, Mulroy SJ, Rao S, Gronley JK, Bontrager EL, The effect of level of spinal cord injury on shoulder joint kinetics during manual wheelchair propulsion. Clin Biomech. 2001;16(9):51-74.

Kulig K, Rao SS, Mulroy SJ, Newsam CJ, Gronley JK, Bontrager EL, Perry J Shoulder joint kinetics during the push phase of wheelchair propulsion. Clin Orthop Relat Res. 1998 Sep;(354):132-143.

Kulig K, Rao SS, Mulroy SJ. Shoulder joint kinetics during the push phase of wheelchair propulsion. Clin Orthop Relat Res Sep 1998;354:132-143.

Kulig, K, Newsam, CJ, Mulroy, SJ. The effect of level of spinal cord on shoulder joint kinetics during manual wheelchair propulsion. Clinical Biomechanics. 2001;16:744-751.

Kwarciak AM, Sisto SA, Yarossi M, Price R, Komaroff E, Boninger ML. Redefining the manual wheelchair stroke cycle: identification and impact of nonpropulsive pushrim contact. Arch Phys Med Rehabil 2009;90:20-26.

Kwarciak AM, Yarossi M, Ramanujam A, Dyson-Hudson TA, Sisto SA. Evaluation of wheelchair tire rolling resistance using dynamometer-based coast-down tests. J Rehabil Res Dev. 2009 46(7): 95-105.

Loslever R Ranaivosoa A. Biomechanical and epidemiological investigation of carpal tunnel syndrome at workplaces with high risk factors. Ergonomics 1993;36:537-555.

Masse LC, Lamontagne M, O'Riain MD. Biomechanical analysis of wheelchair propulsion for various seating positions. J Rehabil Res Dev 1992;29(3):12-28.

Mâsse LC, Lamontagne M, O'Riain MD. Biomechanical analysis of wheelchair propulsion for various seating positions. J Rehabil Res Dev. 1992 Summer;29(3):12-28.

Mercer JL, Boninger M, Koontz A, Ren D, Dyson-Hudson T, Cooper R. Shoulder joint kinetics and pathology in manual wheelchair users. Clin Biomech 2006;21:781-789.

Michael L. Boninger, Rory A. Cooper, Rick N. Robertson, Thomas E. Rudy Wrist biomechanics during two speeds of wheelchair propulsion: An analysis using a local coordinate system Arch Phys Med and Rehabil. April 1997;74(8):364-372

Mulroy SJ, Farrokhi S, Newsam CJ, Perry J. Effects of spinal cord injury level on the activity of shoulder muscles during wheelchair propulsion: an electromyographic study.Arch Phys Med Rehabil. 2004 Jun;85(6):925-934.

Mulroy SJ, Gronley JK, Newsam CJ, Perry J. Electromyographic activity of shoulder muscles during wheelchair propulsion by paraplegic persons. Arch Phys Med Rehabil. 1996 Feb;77(2):187-193.

Mulroy SJ, Newsam CJ, Gutierrez DD, Requejo P, Gronley JK, Lighthall Haubert L, Perry J. Effect of fore-aft seat position on shoulder demands during wheelchair propulsion: part 1. A kinetic analysis. J Spinal Cord Med 2005; 28(3):214-21.

Neer CS, Welsh RP. The shoulder in sports. Orthop Clin North Am 1977;8:583-591.

Newsam C.J., Mulroy S.J., Gronley J.K., Bontrager E.L., Perry J. Temporal-spatial characteristics of wheelchair propulsion: effects of level of spinal cord injury, terrain, and propulsion rate. American Journal of Physical Medicine & Rehabilitation. 1996;75:292–299.

Newsam C.J., Rao S.S., Mulroy S.J., Gronley J.K., Bontrager E.L., Perry J. Three-dimensional upper extremity motion during manual wheelchair propulsion in men with different levels of spinal cord injury. Gait Posture. 1999;10:223–232.

Newsam CJ, Rao SS, Mulroy SJ, Gronley JK, Bontrager EL, Perry J. Three-dimensional upper-limb motion during manual wheelchair propulsion in men with different levels of spinal cord injury. Gait Posture. 1999;10(3):22-32.

Nichols PJ, Norman PA, Ennis JR. Wheelchair user's shoulder? Shoulder Pain in patients with spinal cord legions. Scand J Rehabil Med. 1979; 11:29-32.

Noreau L, Proulx P, Gagnon L, Drolet M, Laramee MT. Secondary impairments after spinal cord injury: a population-based study. Arch Phys Med Rehabil. 2000;79:526-535

Parziale JR. Standard v lightweight wheelchair propulsion in spinal cord injured patients. Am J Phys Med Rehabil 1991;70:76–80.

Pentland WE, Twomey LT. Upper limb function in persons with long term paraplegia and implications for independence. Part 1. Paraplegia 1994,32:211-218.

Preservation of upper limb function following spinal cord injury: a clinical practice guideline for health-care professionals. J Spinal Cord Med. 2005;28(5):434-470.

Rao SS, Bontrager EL, Gronley JK, Newsam CJ, Perry J.Three-dimensional kinematics of wheelchair propulsion. IEEE Trans Rehabil Eng. 1996 Sep;4(3):152-160.

Richter WM, Rodriguez R, Woods KR, Axelson PW. Stroke pattern and handrim biomechanics for level and uphill wheelchair propulsion at self-selected speeds. Arch Phys Med Rehabil. 2007;88:81–87

Richter WM, Rodriguez R, Woods KR, Axelson PW. Stroke pattern and handrim biomechanics for level and uphill wheelchair propulsion at self selected speeds. Arch Phys Med Rehabil 2007;88:81-87.

Richter WM. The effect of seat position on manual wheelchair propulsion biomechanics: a quasi-static model-based approach. Med Eng Phys 2001;23(10):707-12.

Rodgers MM, Gayle GW, Figoni SF, Kobayashi M, Lieh J, Glaser RM. Biomechanics of wheelchair propulsion during fatigue. Arch Phys Med Rehabil. 1994 Jan;75(1):85-93.

Sabick MB, Kotajarvi BR, An KN. A new method to quantify demand on the upper extremity during manual wheelchair propulsion. Arch Phys Med Rehabil 2004;85:1151-1199

Sanderson DJ, Sommer HJ. Kinematic features of wheelchair propulsion. J Biomech. 1985;18(6):423-429.

Sawatzky BJ, Kim WO, Denison I. The ergonomics of different tyres and tyre pressure during wheelchair propulsion. Ergonomics. 2004;47(14):1475-1483.

Senk M, Chèze L. Rotation sequence as an important factor in shoulder kinematics.Clin Biomech 2006;21 Suppl 1:S3-S8.

Shimada SD, Robertson RN, Bonninger ML, Cooper RA. Kinematic characterization of wheelchair propulsion. J Rehabil Res Dev. 1998;35:210–218

Sie IH, Waters RL, Adkins RH, Gellman H. Upper extremity pain in the postrehabilitation spinal cord injured patient. Arch Phys Med Rehabil. 1992;73:44-48.

Sie IH, Waters RL, Adkins RH, Gellman H. Upper extremity pain in the postrehabilitation spinal cord injured patient. Arch Phys Med Rehabil 1992;73:44-8.

Silfverskiold J, Waters RL. Shoulder pain and functional disability in spinal cord injury patients. Clin Orthop. 1991;141-145.

Silverstein BA, Fine LJ, Armstrong TJ. Occupational factors and carpal tunnel syndrome. Am J Ind Med 1987;11:343-358

Sinnott KA, Milburn P, McNaughton H. Factor Associated with thoracic spinal cord injury lesion level and rotator cuff disorders. Spinal Cord. 2000;38:748-753

Stefaniwsky L, Bilowit DS, Prasad SS. Reduced motor conduction velocity of the ulnar nerve in spinal cord injured patients. Paraplegia 1980;18:21-24.

Subbarao JV, Klopfstein J, Turpin R. Prevalance and impact of wrist and shoulder pain in patients with spinal cord injury. J Spinal Cord Me. 1995:18:9-13.

Tun CG, Upton J. The paraplegic hand: electrodiagnostic studies and clinical findings. J Hand Surg [Am] 1988;13:716-719.

van der Woude LH, Hendrich KM, Veeger HE. Manual wheelchair propulsion: effects of power output on physiology and technique. Med Sci Sports Exerc 1988;20:70-78.

van der Woude LH, Veeger DJ, Rozendal RH, Sargeant TJ. Seat height in handrim wheelchair propulsion. J Rehabil Res Dev 1989;26(4):31-50.

van der Woude LH, Veeger HE, Rozendal RH. Propulsion technique in hand rim wheelchair ambulation. J Med Eng Technol. 1989 Jan-Apr;13(1-2):136-141.

van Drongelen S, de Groot S, Veeger HE, Angenot EL, Dallmeijer AJ, Post MW, van der Woude LH. Upper extremity musculoskeletal pain during and after rehabilitation in wheelchair-using persons with a spinal cord injury. Spinal Cord. 2006 Mar;44(3):152-159.

van Drongelen S, van der Woude LH, Janssen TW, Angenot EL, Chadwick EK, Veeger DH. Mechanical load on the upper extremity during wheelchair activities. Arch Phys Med Rehabil. 2005;86:1214-1220.

Vanlandewijck YC, Spaepen AJ, Lysens RJ.Wheelchair propulsion efficiency: movement pattern adaptations to speed changes. Med Sci Sports Exerc. 1994 Nov;26(11):1373-1381.

Veeger HE, van der Woude LH, Rozendal RH. Load on the upper extremity in manual wheelchair propulsion. J Electromyogr Kinesiol. 1991 Dec;1(4):270-280.

Veeger HE, van der Woude LH, Rozendal RH. Wheelchair propulsion technique at different speeds. Scand J Rehabil Med. 1989;21(4):197-203.

Werner RA, Franzblau A, Albers JW, Armstrong TJ. Median mononeuropathy among active workers—are there differences between symptomatic and asymptomatic workers? Am J Ind Med 1998;33:374-378.

Wu G, van der Helm FC, Veeger HE, Makhsous M, Van Roy P, Anglin C, Nagels J, Karduna AR, McQuade K, Wang X, Werner FW, Buchholz B. International Society of Biomechanics. ISB recommendation on definitions of joint coordinate systems of various joints for the reporting of human joint motion--Part II: shoulder, elbow, wrist and hand. J Biomech 2005;38(5):981-992.